A Study in Capture Capability of E2 Phage, Thiolated E2 Phage, or Anti-*Salmonella* Antibody for *Salmonella* Using Magnetoelastic Biosensor Platform

by

Jianguo Xi

A thesis submitted to the Graduate Faculty of
Auburn University
in partial fulfillment of the
requirements for the Degree of
Master of Materials Engineering

Auburn, Alabama
August 4, 2018

Keywords: magneto-elastic biosensor, E2 phage, *Salmonella*, anti-*Salmonella* antibody, physical binding, chemical binding

Approved by

Bryan A. Chin, Chair, Professor of Materials Engineering
Zhongyang Cheng, Professor of Materials Engineering
Pengyu Chen, Assistant Professor of Materials Engineering
Tung-shi Huang, Professor of Poultry Science

Abstract

The magnetoelastic biosensor platform is a superior method that can improve food safety and protect from possible bioterrorism versus conventional culture, nucleic acid-, and immunology-based methods due to low cost, time-savings, convenience, and portability. Although magnetoelastic biosensors have been proven to be one of the most promising methods in the rapid detection of food pathogens, many needs remain such as studying different immobilization methods of bio-molecular recognition elements and the effects of immobilization method on the capture efficiency. This thesis will investigate different methods of immobilizing E2 phage, thiolation E2 phage, and anti-*Salmonella* antibody to improve the performance of the magnetoelastic biosensor platform.

This paper also investigates the effect of different washing techniques on the detection capabilities ME biosensors. Washing is used to remove food particles and salts that are in the food being analyzed and become attached to the biosensor surface. However harsh washing may remove bound target bacteria from the ME biosensor surface, resulting in a lower measured population of the bacteria. Thee different washing methods to maintain captured pathogens on the E2 phage-coated magnetoelastic (ME) biosensors surfaces are investigated. ME biosensors with pre-determined resonance frequencies were exposed to *Salmonella* Typhimurium of $5x10^4$ cfu/mL for 1 h. E2 phage immobilized on the biosensors was responsible for specifically capturing the bacteria. After this capture step, the biosensors were washed using thee different washing methods, pipette washing, magnetic bar washing, and dilution washing. The dilution method was found to result in the highest capture efficiency of the bacteria and the greatest resonance frequency shift of the sensors, which means the lowest loss rate of *Salmonella* Typhimurium.

On the other hand, a milli-scale, free-standing, and wireless biosensor has been prepared using Metglas alloy magnetoelastic (ME) particles. The new coil detector was

used to detect the resonant frequency of ME biosensors by placing biosensors outside the coil boundaries under an external magnetic field. Here, the size of the ME biosensor is 1 x 0.2 x 0.03 mm^3, which is easy to control and has good sensitivity. Biosensors were loaded with filamentous E2 phage using Tris-buffer solution. In this study, *Salmonella* solution was loaded uniformly on the surface of the ME biosensor with population ranging from $5x10^5$ to $5 x10^2$ cfu/mL. The control sensor was a standard ME biosensor without E2 phage. The resonance frequency shift decreased with population of *Salmonella* ranging from $5x10^5$ to $5 x10^2$ cfu/mL. The capture efficiency was detected using plate counting, which demonstrated that the capture efficiency decreased with the population of *Salmonella*, which was positively correlated with the change of the resonance frequency shift. Atomic Force Microscope (AFM) was used to study the binding between filamentous E2 phage or thiolation E2 phage and *Salmonella*. AFM showed that filamentous E2 phages and thiolation E2 phages overlay on the surface of the ME biosensor, and several E2 phages or thiolation E2 phages bound a single *Salmonella* cell simultaneously.

Acknowledgements

I would like to express my gratitude for my advisor Dr. Bryan A. Chin's professional guidance and persistent help during three years' research at Auburn University. Without Dr. Chin's wisdom, patience, and encouragement, I could not finish the thesis successfully. I am also grateful to all my committee members, Dr. Zhongyang Cheng, Dr. Pengyu Chen, and Dr. Tung-shi Huang for their sincere help and support. Special thanks to Dr. Tung-shi Huang for providing the bio-safety laboratory.

I also would like to give my appreciation and sincere thanks to Ms. I-Hsuan Chen for her help in the biological sample preparations and helpful discussions and insightful suggestions. I also thanks Dr. Shin Horikawa for teaching me how to use instruments in Dr. Chin's laboratory and giving me many invaluable suggestions and guidance. Thanks are due to Dr. Majid Beidaghi for his helpful suggestions and guidance in Atomic Force Microscope; Dr. Sang-jin Suh for teaching me very important biological knowledge and giving me generous guidance and kind support; Dr. Edward Davis, Dr. Jeffrey Fergus, Dr. Dong-Joo Kim, Dr. Ruel Overfelt, and Dr. Bart Prorok for insightful guidance and generous support.

Thanks also go to my colleague and friends, Mr. Songtao Du, Mr. Yuzhe Liu, Dr. Yang Tong, Mr. Emre Kayali, Mr. Jafar Orangi, Dr. Xu Lu, and Mr. Jun Chen for all their help and suggestions.

The author would also like to express sincere thanks to his parents and his family for their love, constant emotional support and encouragement during his studies.

Table of Contents

List of Figures

Fig. 5.5 The capture efficiency of biosensors loaded with an anti-Salmonella antibody, the population of which was 2.7 μg/ml. The population of *Salmonella* were 10^2, 10^3,10^4, 10^5 cfu/ml.

List of Tables

Table 5.7 The population of *Salmonella* and anti-*Salmonella* antibody loaded into corresponding 330 µl test tubes. M means measurement biosensors and C means control biosensors.

List of Abbreviations

AFM	Atomic Force Microscopy
AUFDS	Auburn University Detection and Food Safety Center
EDC	1-ethyl-3-(3-dimethylaminopropyl) carbodiimide hydrochloride
EDS	Energy Dispersive X-ray Spectroscopy
ELISA	Enzyme-linked Immunosorbent Assay
FAB	Fragment Antigen Binding Region
FC	Fragment Crystallization Region
HP-NP	Horseradish Peroxidase Nanoparticles
PAB	Polyclonal Antibody
PCR	Polymerase Chain Reaction
SEM	Scanning Electron Microscopy
NHS	N-hydroxy sulfosuccinimide
SWCNT	Single Wall Carbon Nanotu

Chapter 1 Introduction

1.1 Background and need

For humans, food is essential for living and keeping healthy in daily life. However, the recent decades have witnessed a global epidemic in the outbreak of food poisoning and associated illnesses. Some producers believe that it is highly possible for humans to get illnesses, including fatal cases, by consuming contaminated post-harvest plant [1]. During the ready-to-eat food production and preparation process, it is very easy for foods and food products to be contaminated at many points in the food chain. As reported, there are over 2500 serotypes of *Salmonella*, of which *Salmonella enterica serovar typhimurium* (*S.* Typhimurium) and *S. enterica serovar Enteritidis* (*S.* Enteritidis) are the most common serotypes of *Salmonella* to cause human illness associated with ready-to-eat food in western countries [2].

According to data from Center for Disease Control and Prevention (CDC) and Food & Drug Administration, over 1.4 million humans are infected with *Salmonella* annually in the United States, and almost 20,000 humans were hospitalized with nearly 400 deaths [3]. The estimated total cost of *Salmonella* infections is about $2.65 billion annually in 2010, in which the average cost per case is $1896 based on US Department of Agriculture (USDA)'s Economic Research Service (ERS) [4]. Compared with the United States and Europe, there is a higher occurrence in the developing countries, due to lack of advanced testing equipment and fundamental theoretical research. In the developing countries, people generally are deficient in associated knowledge about *Salmonella*.

On average, there are 31 major pathogens reported each year in the United States, which cause about 9.4 million to be infected with foodborne illness. As reported by the Centers for Disease Control and Prevention (CDC) [4], norovirus acts as a major reason for most illness, which accounts for 58%, followed by nontyphoidal *Salmonella* spp., ~11%,

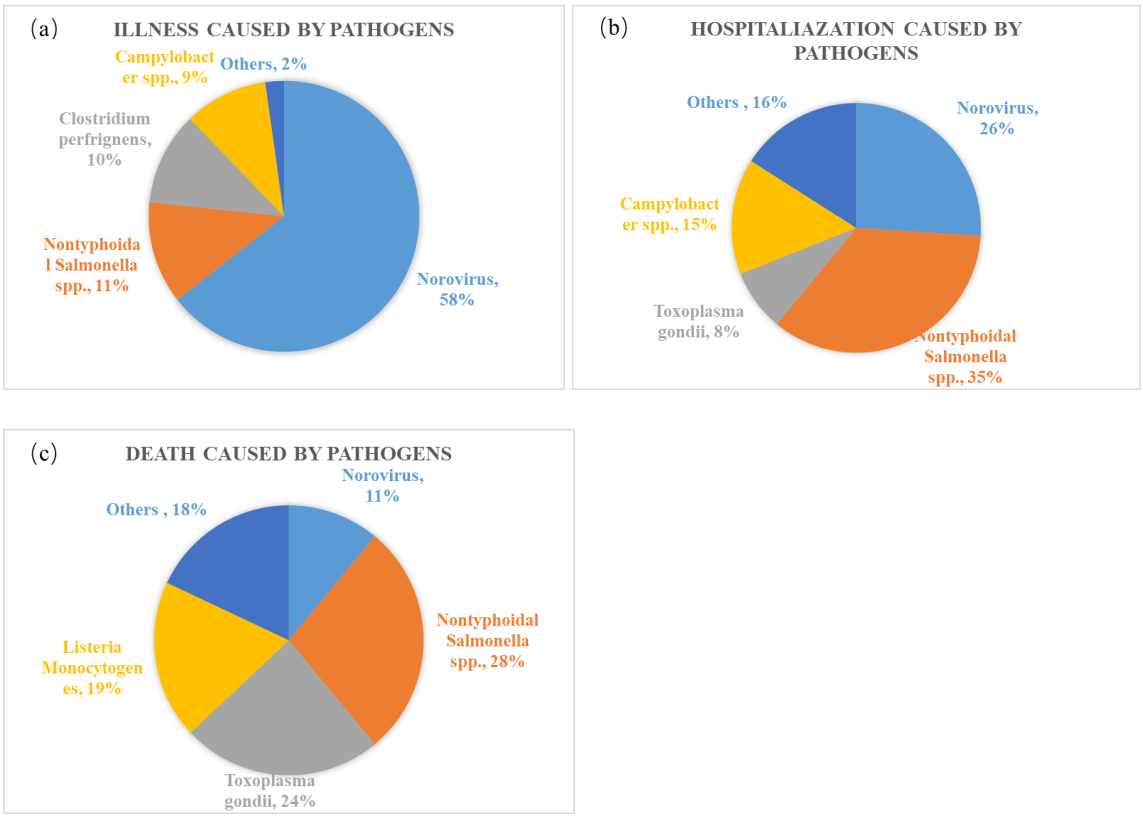

Fig. 1.1 The percentage of illness, hospitalization, and death caused by pathogens reported by Centers for Disease Control and Prevention

Clostridium perfringens, ~10%, and *Campylobacter* spp. ~9%. For hospitalization, nontyphoidal *Salmonella* spp. is the leading cause (35%), followed by norovirus (26%), *Campylobacter* spp. (15%), and *Toxoplasma gondii* (8%). For death, nontyphoidal *Salmonella* spp.is still a primary cause (28%), followed by T. *gondii* (24%), *Listeria Monocytogenes* (19%), and norovirus (11%). The ratios of illness, hospitalization, and death caused by pathogens are presented in Fig. 1. It illustrates that nontyphoidal *Salmonella* accounted for a large part in hospitalization and death caused by pathogens. The bacteria, nontyphoidal *Salmonella*, must be controlled and detected at the food processing plants, transportation centers, grocery stores and restaurants.

Foodborne illnesses caused by pathogens will produce a different economic burden for federal agencies. According to the economic research service of United States Department of Agriculture, 15 major foodborne pathogens will cost the U.S. economy $15.5 billion every year in medical care, and lost productivity (including lost time from work and losses

due to unexpected death) [5]. The ranking top 5 pathogens in cost are *Salmonella*, *Toxoplasma gondii*, *Listeria monocytogenes*, *Norovirus*, *Campylobacter*, which will cost about $13.8 billion, accounting for 89.7% of the total cost of 15 major foodborne pathogens [5]. Of 15 major foodborne pathogens, the cost in illness caused by *Salmonella* is $3.7 billion, which is a huge economic cost in medical care and lost productivities caused by *Salmonella*. It is necessary to design a low-cost, convenient, rapid way to detect *Salmonella* along the entire production, processing, transportation, marketing and consumption food chain.

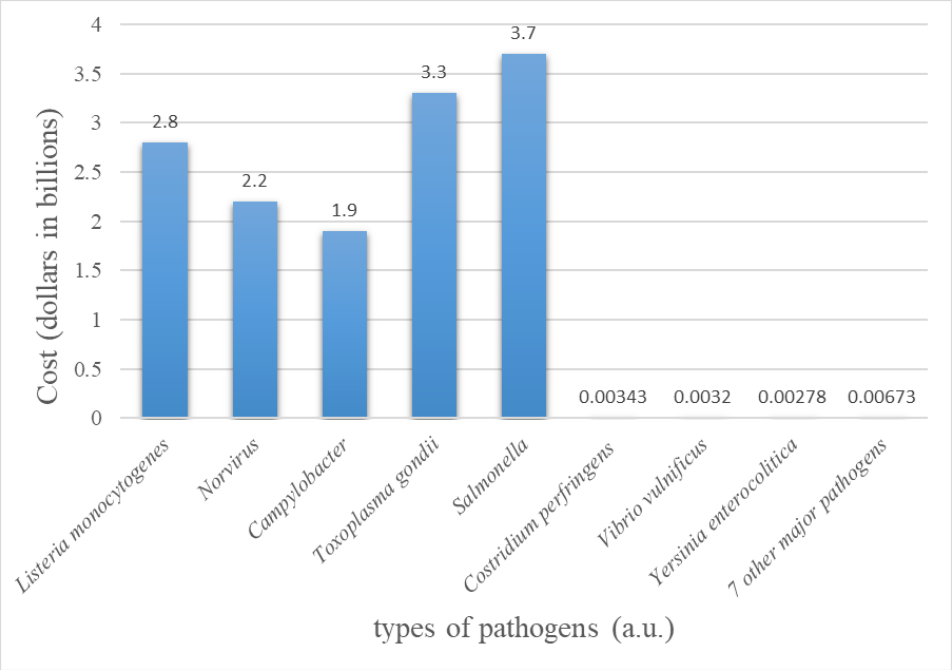

Fig. 1.2 Yearly economic cost of illness caused by 15 major U.S. foodborne pathogens estimated by USDA, Economic Research Service [5].

1.2 *Salmonella*

Salmonella, a group of gram-negative bacteria with elliptically rod shape, is one of the most common causes of food poisoning in the United States. Usually, *Salmonella* is not a type of seriously deadly bacteria, with most people recovering without treatment after being infected with *Salmonella*. But for people with low immunity, including older people, infants, and those with chronic diseases, *Salmonella* is very dangerous. In general, by cooking and other sterilization methods, *Salmonella* will be killed.

Generally, the size of *Salmonella* is 0.7~1.5 μm in diameter and 2~5 μm in length with peritrichous flagella around the *Salmonella* cell body, which is non-spore-forming, as shown in Fig. 1.3 [6]. *Salmonella* cells are hazardous bacteria that exist on the surface of foods, especially fresh vegetables and fruits, and affect human health seriously. *Salmonella* causes gastroenteritis, bacteremia, and subsequent fecal infection [7]. Every year, about 11% of the U.S. population become ill, about 20,000 require hospitalization and 400 deaths occur due to contact with *Salmonella* [4]. Food poisoning, caused by ingesting foods that contain a high population of non-typhoidal *Salmonella* spp., is a common foodborne disease that occurs in most countries today, and is usually contracted from different sources [8], including eggs, meat, poultry, and fresh produce as shown in Table 1.1.

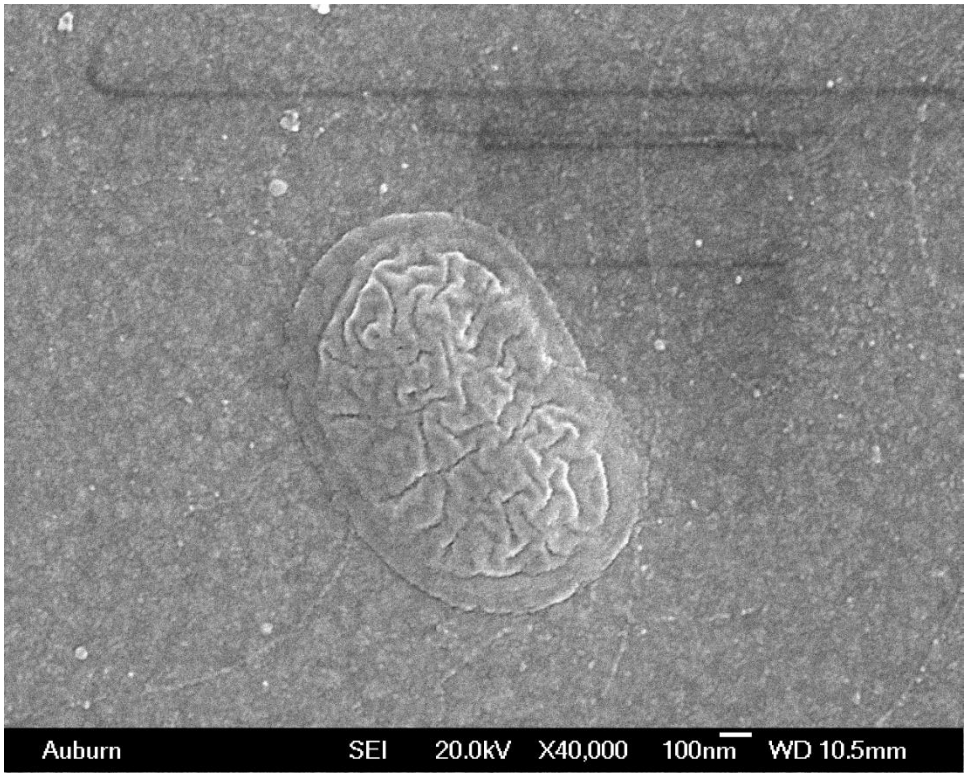

Fig. 1.3 A *Salmonella* cell bound to the surface of a magnetoelastic biosensor after gold coating for SEM imaging.

Table 1.1 Multistate Outbreak of *Salmonella* infections linked to different foods in the U.S.

Produces	*Source*	*Cases*	*Hospitalizations*	*year*	*Ref.*
Shell Eggs	S. Braenderup	35	11	2018	[9]
Dried Coconut	S. Typhimurium	14	3	2018	[10]
Chicken Salad	S. Typhimurium	265	94	2018	[11]
Raw Sprouts	S. Montevideo	10	0	2018	[12]
Pet Guinea Pigs	S. Enteritidis	9	1	2018	[13]
Maradol Papayas	S. Urbana	7	4	2017	[14]
	S. Newport S. Infantis	4	2	2017	[15]
	S. Anatum	20	5	2017	[16]
	S. Thompson S. Kiambu S. Agona S. Gaminara	220	68	2017	[17]
Pet Turtles	S. Agbeni	76	30	2017	[18]
Live Poultry	*Salmonella*	1120	249	2017	[19]
Alfalfa Sprout	S. Abony	62	15	2016	[20]
	S. Muenchen S. Kentucky				[21]
Dairy Calves	S. Heidelberg	56	17	2016	[22]
Organic Shake& Meal Products	S. Virchow	33	6	2016	[23]
Shell Eggs	S. Oranienburg	8	2	2016	[24]
Cucumbers	S. Poona	907	204	2015	[25]
Raw, Frozen, Stuffed Chicken Entrees	S. Enteritidis	5	2	2015	[26]
Pet Crested Geckos	S. Muenchen	22	3	2015	[27]
Pork	S. Infantis	192	30	2015	[28]

1.3 Bacteriophages to be used

Bacteriophage, or phage, is a virus that infects and replicates within bacteria cells. Generally, phage has a very simple structure, which is composed of proteins that

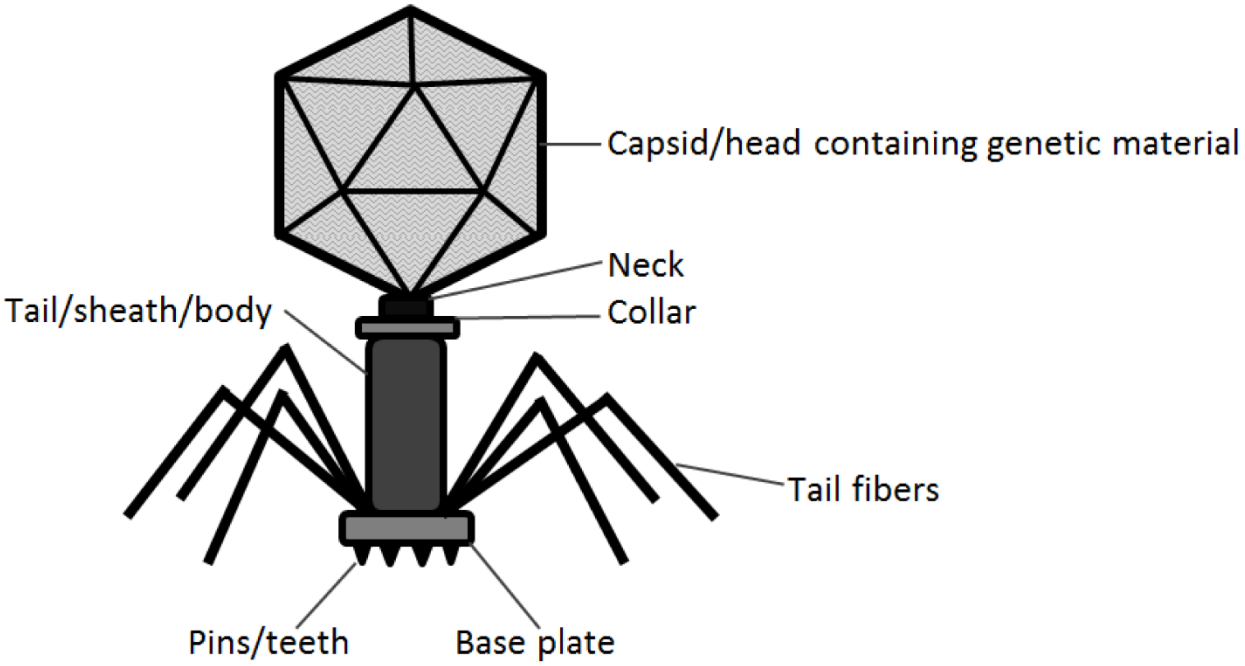

Fig. 1.4 Schematic illustration of one typical bacteriophage [29]

1.3.1 E2 phage

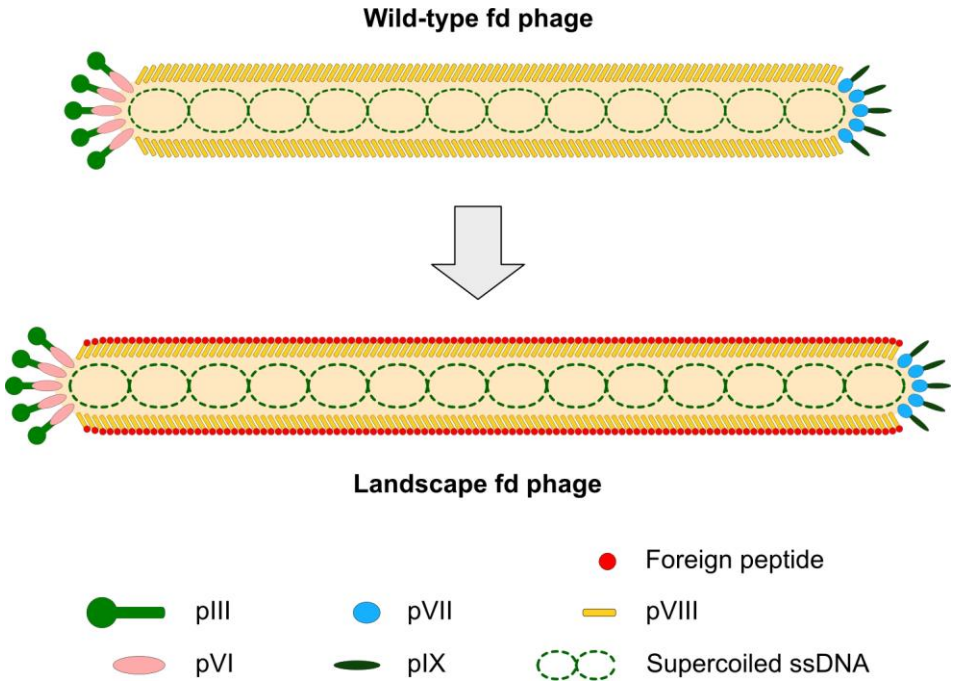

Fig. 1.5 Schematic diagram of the wild-type fd phage and fd phage modified via genetically engineering with a foreign peptide loading on the main coat protein pVIII [32].

encapsulate DNA or RNA genome. These genomes can encode 4 genes at least, which will be injected into the cytoplasm, as shown in Fig. 4 [29].

E2 phage is one bacteriophage, modified via genetically engineering using phage display technology [30-31], as shown in Fig. 1.5 [32]. The top one is wild-type fd phage, and the bottom one is wild-type fd phage modified via genetically engineering with one foreign peptide on the main coat protein pVIII. Generally, the wild-type fd phage strains with the identical DNA sequences are flexible and thead-like particles, which have 800~1,000 nm in length and 7 nm in diameter [33]. One normal fd phage contains the major coat protein from phage gene VIII, several minor coat proteins, such as A protein from gene III, polypeptide from gene V, and so on. Gene VIII forming the major coat protein has only 49 amino acids, while there are about 2,000 copies per virion for the major coat protein, which accounts for 98% molecular weight of the total weight of fd phage [34].

Table 1.2 The sequences of amino acids of the fd coat protein from different genes. The underlined part is the hydrophobic domains, whereas "+" indicates positive charge and "-" indicates negative charge.

Proteins	*Sequence of amino acids*
pVIII	AĒGD̄D̄PAKAAFD̄SLQASATĒYIGYAWAMVVVIV GATIGIKLFKKFTSKAS
pIII	FRGVFFLLYVATFMYVFSTFANILRNKĒS
pVI	MPVLLGIPLLLRFLGFLLVTLFGYLLTFLKKGFG K IAIAISLFLALIIGLNSILVGYLSD̄ISAQLPSD̄FVQG VQLILPSNALPCFYVILSVKAAIFIFD̄VKQK IVSYLD̄QD̄K
pVII	MĒQVAD̄FD̄TIYQAMIQISVVLCFALGIIAGGQR
pIX	MSVLYYSFASFVLGWCLRSGITYFTRLMĒTSS

Every copy of the minor coat proteins includes two ends, pIII or pVI at one end, and pVII or pIX at the other end, as shown in Table 1.2, which illustrates the sequences of amino acid of the fd coat proteins, such as pVIII, pIII, pVI, pVII, and pIX. One or several hydrophobic domains exist within the interior sequence of amino acid, for example, the major coat protein pVIII has a hydrophobic domain with one continuous amino acid strain (YIGYAWAMVVVIVGATIGI) within the amino acid sequence, which connected with adjacent copies via hydrophobic interaction between these domains [35]. In order to keep a charge balance, residues with positive charge near the C-terminus will interact with DNA with negative charges. The major coat protein pVIII may interact with the minor coat proteins pIII, pVI, and pVII within phage, in which pIII and pIX proteins are exposed to the environment, and pVI and pVII proteins are not [36].

These wild-type Ff phages are viruses, which infect *E. Coli* (*Escherichia coli*) via F pili or attach the N terminal domains of the pIII protein to the tip of pilus [31]. Then, the coat proteins are dissolved into the surface of the bacteria, and Ff phages release viral DNA into the cytoplasm of bacteria, where a large amount of offspring viral DNA molecules are synthesized mechanically within the host cells. Subsequently, these viral DNA molecules acquire the coat proteins from the membrane of bacteria cells in the process of extrusion, and new independent virions form. Every division may secrete up to 1,000 virions increasing without killing the host cells, and the entire divisions can yield more than 0.3 mg/ml. In this research, E2 phage was derived from the landscape phage libraries f8/8 and f8/9 [37], displaying foreign octamers or nanomers in approximately 4,000 copies of the major coat protein pVIII, and chosen as the biomolecular recognition elements. Octamer means thee amino acid residues (EGD) of the wild-type pVIII are substituted by a random octamer in the f8/8 library, in which a random octamer can be any amino acid residue, while nanomer means four amino acid residues (EGDD) of the wild-type pVIII are substituted by a random nanomer in the f8/9 library. One part of amino acid sequence in pVIII was exposed to the ambience, when the other part was buried in the capsid. For E2 phage, the foreign peptide sequence exposed to the ambience is VTPPTQHQ, which aims at *Salmonella* as a target [38].

1.3.2 Thiolated E2 phage

Traut's Reagent (2-Iminothiolane or 2-IT) is one cyclic thioimidate compound to add sulfhydryl (-SH) to the target phage, which can help E2 phage build one strong bonding with gold layer. The principal for thiolation using Traut's Reagent is that Traut's Reagent reacts with primary amines ($-NH_2$) so that sulfhydryl groups were introduced into the E2 phage, maintaining charge balance which is similar to the original amino group, as shown in Fig. 1.6 [39]. Once thiolated, E2 phage may be specifically and stably connected with gold layer via sulfhydryl group.

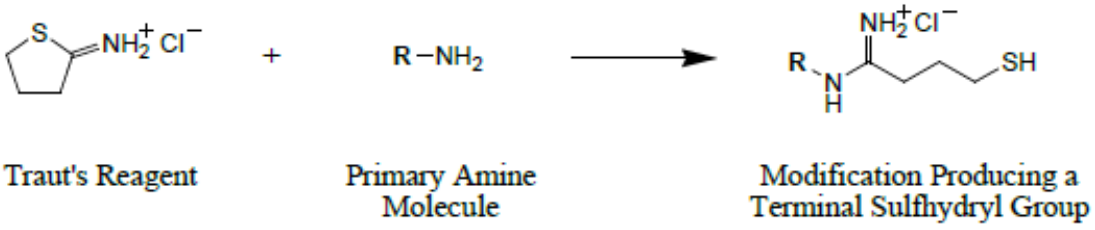

Fig. 1.6 Schematic illustration of reaction between Traut's Reagent and primary amine molecule

1.4 Anti-*Salmonella* Antibody

During the past decades, anti-*Salmonella* antibodies were the most common biomolecular recognition element, which is one IgG-type molecule with a Y shape. In order to use the antibody as a biomolecular recognition element, many factors must be considered, such as thermal stability, selectivity, and production cost [40,41], which will restrict the application of antibody. Recently, as one alternative, landscape phages have attracted more attention, which have been applied to various bio-sensing systems [42-45]. Table 1.3 shows the difference in the life span between a landscape phage and monoclonal antibody specifically for β-galactosidase at different temperatures [40]. As shown in Table 1.3, both landscape phage and antibody can retain normal binding activity at room temperature. However, as temperature increases, antibody loses the binding activity faster than that of landscape phage. When selecting a suitable biomolecular recognition element, thermal stability is a critical factor to be considered. At the higher temperatures, antibodies are not a good choice for biomolecular recognition.

Table 1.3 Life span of a landscape phage and monoclonal antibody specifically for β-galactosidase at different temperatures [40]

Temperature	*Landscape phage*	*antibody*
Room temperature	More than 180 days	More than 180 days
37 ℃	~950 days	~107 days
50 ℃	~35 days	~35 days
63 ℃	~42 days	1 day
76 ℃	~2.4 days	0

In addition, it is necessary to compare the selectivity and production cost between landscape phage and antibody, as shown in Table 1.4 [32]. By contrast, the production cost for antibodies is higher, which is not a very economic biomolecular recognition element. For selectivity, landscape phage and monoclonal antibodies have high selectivity.

Table 1.4 Selectivity and production cost for landscape phage and antibodies [32]

Recognition element	*Selectivity*	*Production cost*	*Reference*
Landscape phage	High	Low	[40-42]
Monoclonal antibodies	High	Very high	[40, 43]
Polyclonal antibodies	Low	high	[40, 43]

1.5 Research motivation

Magnetoelastic (ME) biosensors are potential candidates that can be used in a biosensing system, because of its low-cost, convenience, portablity, and mass-sensitive properties. The Auburn University Detection and Food Safety Center (AUDFS) has researched detection using freestanding, strip-shaped ME biosensors loaded with E2 phage for many years. However, very little of the past research has addressed the issue of how to improve the capture efficiency of the biosensor. Recently, our attentions have focused on the relationship between capture capability of ME biosensor, binding times of *Salmonella* and E2 phage, and method of washing that avoid removing *Salmonella* from the phage. In addition, it is necessary to obtain a highly efficient molecular recognition element by

comparing E2 phage, thiolated E2 phage, and anti-*Salmonella* antibody in capture efficiency. In this experiment, resonance frequency shifts were measured using the surface-scanning detection method, capture efficiency was measured using the plate counting method, and morphology of the ME biosensor when combined with E2 phage, thiolation E2 phage, or anti-*Salmonella* antibody and *Salmonella*.

1.6 Thesis organization

In this chapter, the necessity to compare the difference among E2 phage, thiolated E2 phage, and anti-*Salmonella* antibody in resonance frequency shift or mass sensitivity, and capture efficiency was described, and the objectives of the current research were stated.

Chapter 2 briefly describes major bacterial detection methods.

Chapter 3 describes the washing methods of phage-based ME biosensors and binding time between E2 phage and *Salmonella*.

Chapter 4 presents results from an investigation into the resonance frequency shift and capture efficiency of ME biosensors combined with E2 phage and thiolation E2 phage using wireless, free-standing biosensors, and observation of the morphology of ME biosensor surfaces.

Chapter 5 illustrates the relationship between anti-*Salmonella* antibody and E2 phage with population of *Salmonella*, and the procedures of anti-*Salmonella* antibody preparation. An investigation into the resonance frequency shift and capture efficiency of ME biosensors combined with anti-*Salmonella* antibody using wireless, free-standing biosensors is presented, and the morphology of ME biosensor surface with anti-*Salmonella* antibody is observed.

Chapter 6 presents a comprehensive summary and conclusions for this thesis.

Bibliography

[1] M. L. L. Ivey, J. T. LeJeune, S. A. Miller. “Vegetable producers’ perceptions of food safety hazards in the Midwestern USA”. Food Control, vol. 26, no. 2, pp. 453-465, 2012.

[2] J. Fierer, and D. G. Guiney. “Diverse virulence traits underlying different clinical outcomes of *Salmonella* infection”. Journal of Clinical Investigation, vol. 107, no. 7, pp. 775-780, 2001.

[3] K. J. Cummings, L. D. Warnick, M. Elton, Y. T. Grohn., P. L. McDonough, and J. D. Siler. “The effect of clinical outbreaks of *Salmonellosis* on the prevalence of fecal *Salmonella* shedding among dairy cattle in New York”. Foodborne Pathogens and Disease, vol. 7, no. 7, pp. 815-823, 2010.

[4] http://www.cidrap.umn.edu/news-perspective/2010/05/

[5]https://www.ers.usda.gov/data-products/chart-gallery/gallery/chart-detail/?chartId=88113

[6]http://www.foodpoisonjournal.com/foodborne-illness-outbreaks/washington-pork-salmonella-outbreak-hits-134/

[7] S. J. Chai, P. L. White, S. L. Lathop, S. M. Solghan, C. Medus, B. M. Mcglinchey, M. T. D’Angelo, R. Marcus, and B. E. Mahon. Salmonella enterica Serotype Enteritidis: increasing incidence of domestically acquired infections, *Clinical Infectious Diseases*, vol. 54, pp. S488-S497, 2012.

[8] S. K. Eng, P. Pusparajah, N. S. A. Mutalib, H. L. Ser, K. G. Chan, and L. H. Lee. Salmonella: a review on pathogenesis epidemiology and antibiotic resistance, Frontiers in Life Science, vol. 8, pp. 284-293, 2014.

[9] CDC, https://www.cdc.gov/salmonella/braenderup-04-18/index.html, 2018.

[10] CDC, https://www.cdc.gov/salmonella/typhimurium-03-18/index.html, 2018.

[11] CDC, https://www.cdc.gov/salmonella/typhimurium-02-18/index.html, 2018.

[12] CDC, https://www.cdc.gov/salmonella/montevideo-01-18/index.html, 2018.

[13] CDC, https://www.cdc.gov/salmonella/guinea-pigs-03-18/index.html, 2018.

[14] CDC, https://www.cdc.gov/salmonella/urbana-09-17/index.html, 2018.

[15] CDC, https://www.cdc.gov/salmonella/newport-09-17/index.html, 2018.

[16] CDC, https://www.cdc.gov/salmonella/anatum-9-17/index.html, 2018.

[17] CDC, https://www.cdc.gov/salmonella/kiambu-07-17/index.html, 2018.

[18] CDC, https://www.cdc.gov/salmonella/agbeni-08-17/index.html, 2018.

[19] CDC, https://www.cdc.gov/salmonella/live-poultry-06-17/index.html, 2018.

[20] CDC, https://www.cdc.gov/salmonella/reading-08-16/index.html, 2018.

[21] CDC, https://www.cdc.gov/salmonella/muenchen-02-16/index.html, 2018.

[22] CDC, https://www.cdc.gov/salmonella/heidelberg-11-16/index.html, 2018.

[23] CDC, https://www.cdc.gov/salmonella/virchow-02-16/index.html, 2018.

[24] CDC, https://www.cdc.gov/salmonella/oranienburg-10-16/index.html, 2018.

[25] CDC, https://www.cdc.gov/salmonella/poona-09-15/index.html, 2018.

[26] CDC, https://www.cdc.gov/salmonella/frozen-chicken-entrees-part2-07-15/index.html, 2018.

[27] CDC, https://www.cdc.gov/salmonella/muenchen-05-15/index.html, 2018.

[28] CDC, https://www.cdc.gov/salmonella/pork-08-15/index.html, 2018.

[29] J. Doss, K. Culbertson, D. Hahn, J. Camacho, and N. Barekzi. “A review of phage therapy against bacterial pathogens of aquatic and terrestrial organisms”. Viruses, vol. 9, no. 3, pp 50, 2017.

[30] V. A. Petrenko, G. P. Smith, X. Gong, and T. Quinn. A library of organic landscapes on filamentous phage, *Protein Engineering*, vol. 9, pp. 797-801, 1996.

[31] G. P. Smith and V. A. Petrenko, Phage display, *Chemical Reviews*, vol. 97, pp. 391-410, 1997.

[32] S. Horikawa. Low cost, rapid, sensitive detection of pathogenic bacteria using phage-based magnetoelastic biosensors, 2013.

[33] K. Li, Y. Chen, S. Q. Li, H. G. Nguyen, Z. W. Niu, S. J. You, C. M. Mello, X. B. Lu, and Q. Wang. Chemical modification of M13 bacteriophage and its application in cancer cell imaging, *Bioconjugate Chemistry*, vol. 21, pp. 1369-1377, 2010.

[34] T. J. Henry and D. Partt. The proteins of bacteriophage M13, *PNAS*, vol. 62, pp. 800-807, 1969.

[35] D. Marvin. Filamentous phage structure, infection and assembly, Current Opinion in Structural Biology, vol. 8, pp. 150-158, 1998.

[36] H. Endemann and P. Model. Location of filamentous phage minor coat proteins in phage and in infected cells, Journal of Molecular Biology, vol. 250, pp. 496-506, 1995.

[37] G. Kuzmicheva, P. Jayanna, I. Sorokulova, and V. A. Petrenko. Diversity and censoring of landscape phage libraries, Protein Engineering, Design and Selection, vol. 22, pp. 9-18, 1995.

[38] I. B. Sorokulova, E. V. Olsen, I. H. Chen, B. Fiebor, J. M. Barbaree, V. J. Vodyanoy, B. A. Chin, and V. A. Petrenko. Landscape phage probes for *Salmonella typhimurium*, *Journal of Microbiological Methods*, vol. 63, pp. 55-72, 2005.

[39]https://assets.thermofisher.com/TFS-Assets/LSG/manuals/MAN0011238_Trauts_Reag_UG.pdf

[40] V. A. Petrenko, Landscape phage as a molecular recognition interface for detection devices, *Microelectronics Journal*, vol. 39, pp. 202-207, 2008.

[41] S. Goodchild, T. Love, N. Hopkins, and C. Mayers. Engineering antibodies for biosensor technologies, *Advances in Applied Microbiology*, vol. 58, pp. 185-226, 2005.

[42] V. A. Petrenko and I. B. Sorokulova. Detection of biological theats, a challenge for directed molecular evolution, *Journal of Microbiological Methods*, vol. 58, pp. 147-168, 2004.

[43] C. Mao, A. Liu, and B. Cao. Virus-based chemical and biological sensing, *Angewandte Chemie International Edition*, vol. 48, pp. 470-477, 2007.

[44] R. S. Lakshmanan, R. Guntupalli, J. Hu, D. J. Kim, V. A. Petrenko, J. M. Barbaree, and B. A. Chin. Phage immobilized magnetoelastic sensor for the detection of Salmonella typhimurium, *Journal of Microbiological Methods*, vol. 71, pp. 55-60, 2007.

[45] V. A. Petrenko, G. P. Smith, X. Gong, and T. Quinn. A library of organic landscapes on filamentous phage, *Protein Engineering*, vol. 9, pp. 797-801, 1996.

Chapter 2 Literature Review for Bacteria Detection Methods

This chapter reviews currently used bacteria detection methods and describes why alternative methods of detection (biosensors) are needed. Additionally, different types of biosensors and their advantages and disadvantages are discussed.

2.1 Conventional Culture Methods

Conventional culture methods to isolate and identify target bacteria are dependent on whether some bacteria are capable of surviving and growing into visible colonies using a well-defined culture medium. A colony is assumed to derive from one single bacterial cell which can be used to identify the exact number of bacterial cells via counting the number of colonies, as shown in Fig. 2.1. Generally, it will take 5 to 7 days to complete the whole

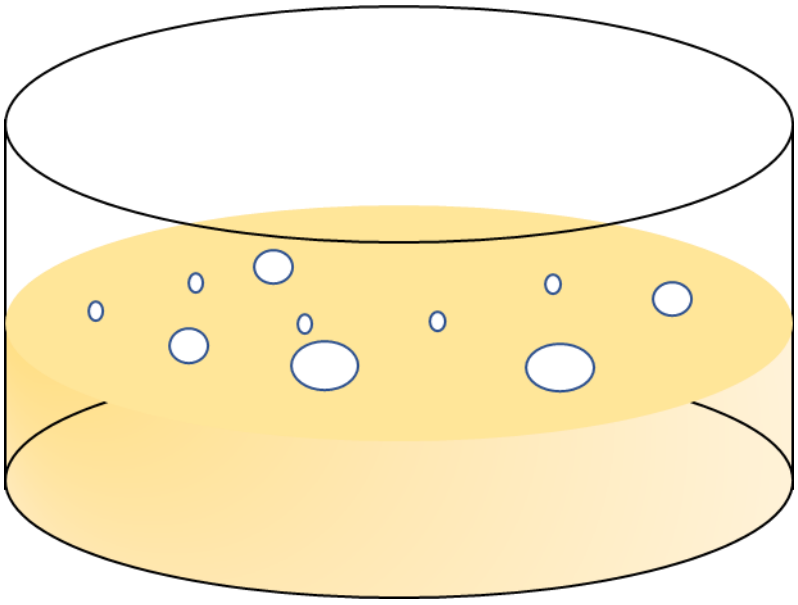

Fig. 2.1 Bacteria colonies on the well-defined culture medium

procedure, which includes pre-enrichment, selective enrichment, biochemical screening, and serological confirmation [1]. In addition, some viable bacteria may enter the dormant state in the environment, and it is almost impossible to be cultured, resulting in

underestimating the quantity of bacteria or failing to identify the existence of bacteria in the sample.

2.2 Molecular Recognition Methods

2.2.1 Nucleic Acid-Based Detection (PCR)

Polymerase chain reaction (PCR) method is used to amplify a certain quantity of genetic material to identify the presence of target bacteria, including *Salmonella aureus*, *Escherichia* [2]. Generally, genetic material is deoxyribonucleic acid (DNA), which is more stable than ribonucleic acid (RNA). The normal PCR procedures contain a series of 20 to 40 thermal cycles, as shown in Fig. 2.2, in which each cycle has thee independent temperature stages [3]:

(1) Denaturation is a process that separates a double-stranded DNA into a couple of single-stranded DNA templates at the temperature of about 95 ℃.

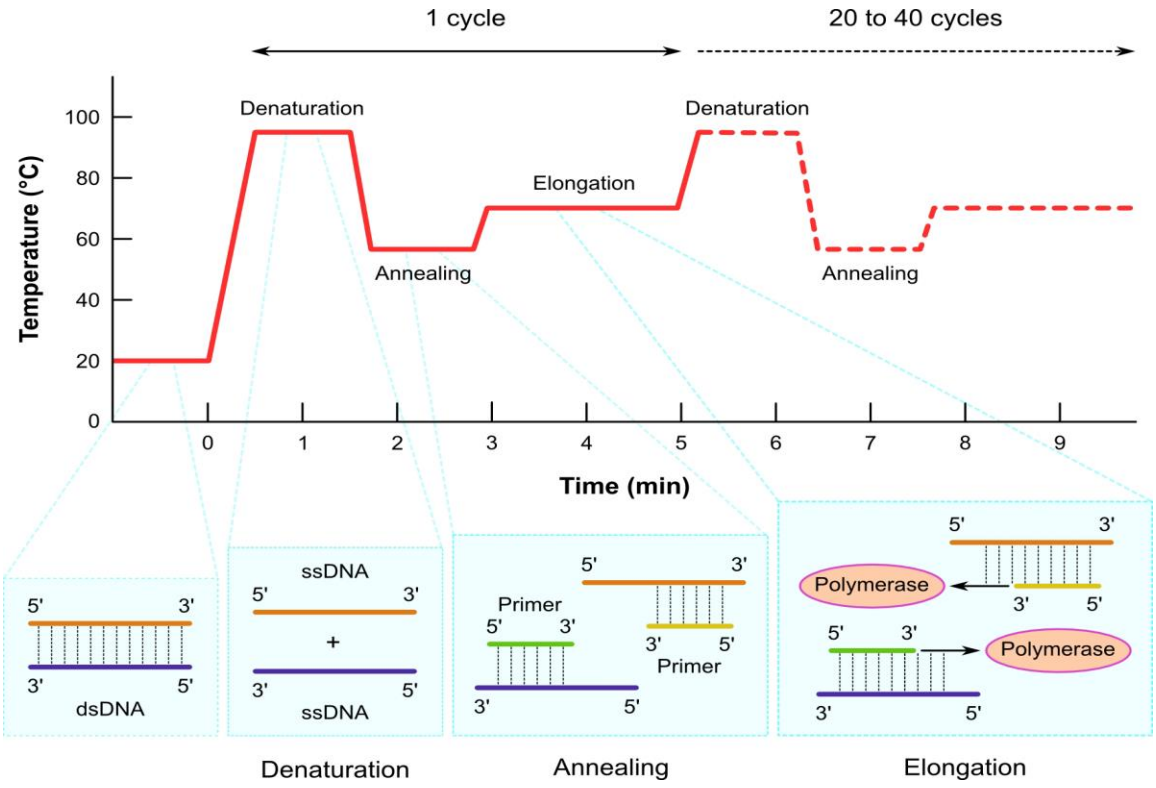

Fig. 2.2 Schematic illustration of polymerase chain reaction (PCR) cycle [3].

(2) Annealing is a process in which forward and reverse primers are allowed to be annealed into single-stranded DNA templates at the temperature of 60±5 ℃.

(3) Elongation is a process in which complementary strands are synthesized via extending the primers under the help of DNA polymerase at the temperature of around 70 ℃.

PCR method is a straightforward method with high specificity and accuracy to detect a small amount of target DNA [4-5]. Under each cycle, amplicons are doubled in quantity, which is used to increase the amount of the target DNA sequence exponentially. Every cycle just costs several minutes, so thousands or millions of target DNA sequence are duplicated within several hours. Finally, the PCR products are analyzed using gel electrophoresis. By contrast, PCR can save more time than that of conventional culture methods. However, PCR is also a complicated way to detect the bacterial with procedures, such as specific primers which is used to avoid amplifying false amplicons, high costs in reagents (for example, DNA polymerase, deoxynucleotide triphosphate or dNTP, and other additives), dozens of thermal cycles, analyzing the amplicons via gel electrophoresis after previous processes. Although novel PCR techniques, such as real-time PCR [6], digital PCR [7], and microfluidic PCR [8], can be advantageous in terms of assay time with less reagent volume, these PCR variants offer some higher requirements, such as the use of a fluorescent-labeled DNA probe and optical detector which is used to acquire the fluorescence signals. Undoubtedly, these additional variants will cause an increase in cost and assay complexity.

2.2.2 Immunology-Based Detection (ELISA)

Another common method is enzyme-linked immunosorbent assay (ELISA), which has been developed and employed widely for detection of bacteria [9-11], such as *Escherichia coli* and *Salmonella* spp. Fig. 2.3 presents a typical protocol for sandwich ELISA [12]. In the protocol, ELISA needs a primary antibody and an enzyme conjugated secondary antibody.

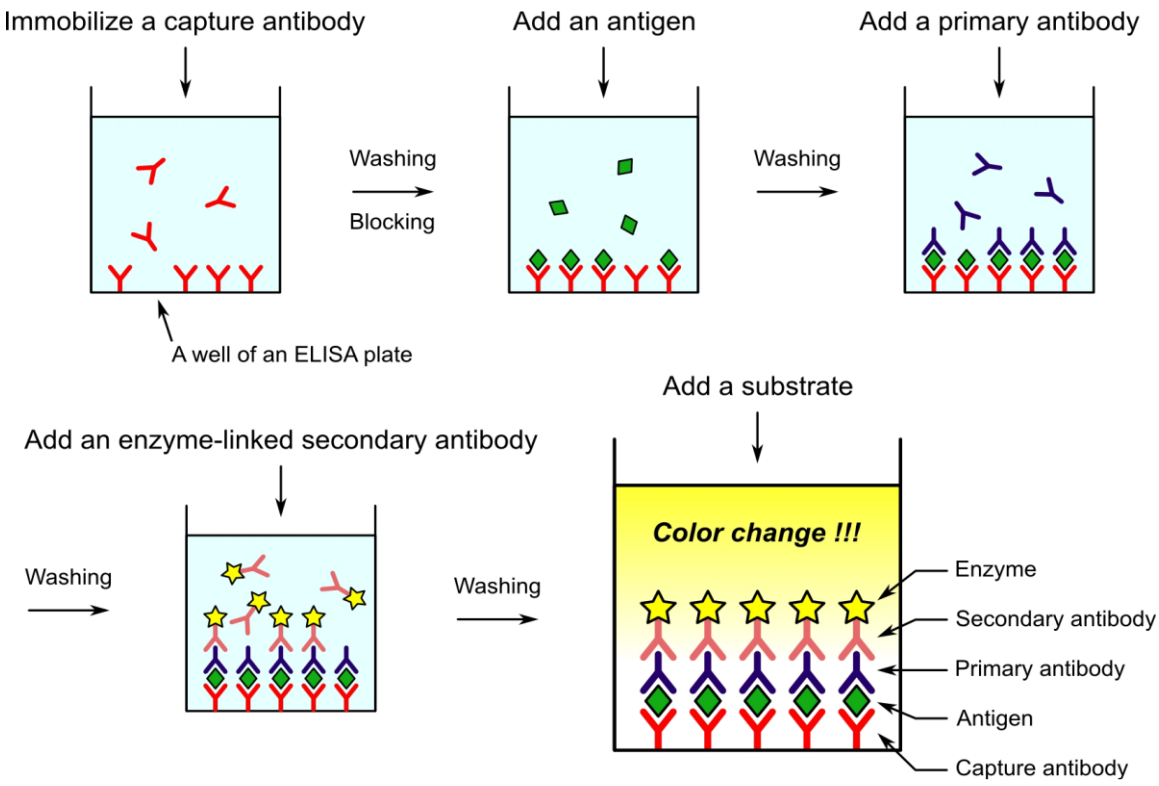

Fig. 2.3 Schematic illustration of enzyme-linked immunosorbent assay (ELISA) [11].

(1) A capture antibody is immobilized on the surface of ELISA plate and incubate the ELISA plate is incubated on the rocker at the rate of 4 rpm for 1 h. Then DI water is used to wash the plate in order to remove any unbound antibodies.

(2) A blocking agent is used to block any unbound adsorption sites on the surface of each well.

(3) A sample with a target antigen is added into each well, in which antigen will bind toa specific antibody, and incubate the ELISA plate is on a incubated rocker at the rate of 4 rpm for 1 h. Then, DI water is used to remove the unbound antigens.

(4) A primary antibody is added into each well and binds with target antigens. Then the ELISA plate is incubated on the rocker at the rate of 4 rpm for 1 h. After incubation, the ELISA plate is washed using DI water to remove unbound primary antibody.

(5) An enzyme-linked secondary antibody is added into each well and binds with the primary antibodies. Then the ELISA plate is incubated on the rocker at the rate of 4 rpm

for 1 h. After incubation, the ELISA plate is washed using DI water to remove unbound primary antibody.

(6) One substrate is added into each well, which will react with enzyme and be converted into a color or electrochemical signal for measurement.

By contrast, the ELISA method, which just requires hours to days for results, takes less time than conventional culture methods [13]. In addition, cumbersome assay procedures reduce the competition of the ELISA method, which enables the ELISA method to be used on-site for bacterial detection. Table 2.1 shows the comparison of limits of detection (LODs) for *Salmonella* among conventional culture, PCR, and ELISA methods.

Table 2.1 Comparisons in LODs for *Salmonella* among conventional culture, PCR, and ELISA methods

Detection Methods	*LOD*	*Assay time*	*Ref.*
conventional culture method	down to 1 cfu/ml	4-8 days	[14]
PCR method	1 cfu/ml	Hours	[15]
ELISA method	10^6 cells/ml	Hours to days	[16]

2.3 Biosensors

A biosensor is a device that converts changes induced by bioactivities of microorganism into electrical signal. Generally, a biosensor is comprised of two fundamental components: a biomolecular recognition element and a signal transducer. A biomolecular recognition element is a medium that can identify and capture specifically a target analyte, while a signal transducer is a device used to convert invisible bioactivities of microorganism into an identifiable signal. For biomolecular recognition element, biosensors can be loaded with antibodies, nucleic acid, enzyme, and/or landscape phage. For signal transducer, biosensors can be mainly classified into electrochemical, optical, and acoustic wave biosensors.

2.3.1 Electrochemical Sensors

So far, electrochemical sensors are the techniques that transfer the interaction between the target analyte and the recognition element into a measurable electrical signal, which

can be applied in multiple fields, such as clinical diagnosis, biochemical analysis, and environmental monitoring [17-19]. Electrochemical sensors are a rapid and low-cost device, which are immobilized on the surface of the electrode using biologically active materials, for example, enzymes or antibodies. Though metabolism of microorganisms, substances without charges or with a small amount of charges, such as carbohydrates, fats or proteins, were transformed into highly charged terminal products, such as organic acids, fatty acids, and amino acids, resulting in forming an electric current within the bio-medium. Based on signals received by a detector, electrochemical biosensors can be classified into impedimetric, conductometric, potentiometric, and amperometric biosensors. Impedimetric biosensors employ the conductivity change of the medium as signal, which can be measured via a bridge circuit, during the process of metabolism of microorganism [20]. Conductometric biosensors are based on the conductance changes caused by biological component between two metal electrodes [21-22]. Potentiometric and amperometric biosensors are two common devices of electrochemical biosensors. A potentiometric biosensor is one that receives an analytical signal via converting the biorecognition process into a measured potential signal at the equilibrium conditions [23-24]. An amperometric biosensor is one that measures current changes though oxidation and reduction of an electroactive substance at two electrodes under a constant applied potential, which have a high sensitivity, rapid response, large measure limit and low cost [25].

2.3.2 Optical Sensors

Optical biosensors are those that employ photons as the signals via measuring absorbance, reflectance, or fluorescence emissions excited by ultraviolet (UV), visible, or near-infrared (NIR), which are different with signals from electrons in the electrochemical sensors. Fluorescence emissions are the most common signal in optical biosensors, in which intensity, decay time, luminescence energy transfer, anisotropy, and quenching efficiency are the main detection parameters. Fluorescence biosensors can be measured in thee ways: the difference in molecules was detected before and after a reaction in direct sensing; the evolution in fluorescence intensity of analyte after a dye added into the solution was detected in the indirect sensing [26]; in addition, an energy change was

detected during the reaction in the fluorescence energy transfer [27]. Optical sensors can be almost measured in situ, which is superior to electrochemical biosensors.

Surface plasmon resonance (SPR) is based on excitation of surface plasmons of optical sensors, which is prepared according to *Kretschmann* configuration in geometrical size, as shown in Fig. 2.4 [28]. Surface plasmon resonance (SPR) is used to detect the evolution in constants of surface plasmons, such as coupling angle, coupling wavelength, intensity, and phase, which is caused via changing the refractive index of the dielectric materials at the specific coupling conditions. Generally, a surface plasmon was excited though the monochomatic light, and the coupling strength caused by incident wave and surface plasmons is better to be detected by utilizing the convergent light beam. About the limit of detection (LOD), proteins with nanomolar population or even smaller level can be detected. For *Escherichia coli* O157:H7, the limit of detection can be 10^2 cells/ml [29].

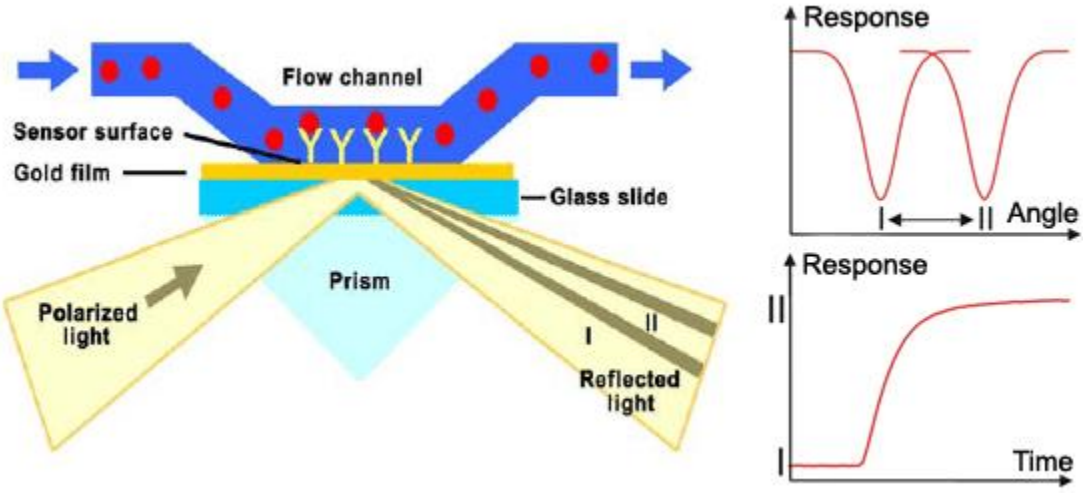

Fig. 2.4 Schematic illustration of surface plasmon resonance-based sensors [28]

Immobilizing antibodies on the sensor, the limit of detection for *Escherichia coli* O157:H7 can be down to 10^2 cells/ml [30]. In addition, Choi's group found the LOD of Salmonella typhimurium can be detected at the population of 10^2 cells/ml when immobilizing protein G at the surface of sensors [31].

2.3.3 Acoustic Wave Biosensors

Acoustic wave sensors are based on changes in elastic or mechanical waves, caused by mass addition on the surface of solid biosensor, which can be detected via measuring the frequency shift of the sensor platform. Generally, biomolecular recognition elements are loaded on the biosensor, which can be used to capture the analyte. The qualities of mass-based biosensors are very sensitive to mass change, economical, and portable. Acoustic wave sensors can be classified into thickness shear acoustic wave sensors, surface acoustic wave sensors and shear-horizontal acoustic wave sensors. Thickness shear acoustic sensors are comprised of piezoelectric materials which can mechanically vibrate under electric field [32]. Surface acoustic wave sensors are sensitive to surface perturbation caused by analyte, which can give rise to a specific acoustic wave propagation at the surface and are monitored via wave shift and attenuation response [33]. Shear-horizontal acoustic wave sensors are based on a thin piezoelectric film at the surface of sensor, which can confine an acoustic waveguide along the surface of sensor and are sensitive to the thickness of the sensors [34].

Table 2.2 Comparisons in LODs for *Salmonella* among electrochemical biosensors, optical biosensors, and acoustic wave biosensors

Detection method		*LOD*	*Assay time*	*Ref.*
Electrochemical biosensors	Impedimetric	2 cells/ml	45 min	[20]
	Conductometric	60 cells/ml	8 min	[21-22]
	Potentiometric	10 to 10^3 cells/ml	30 min to 1.5 h	[23-24]
	Amperometric	10 to 10^3 cells/ml	Minute to hour	[25]
Optical biosensors	Surface plasmon resonance	50 to 10^5 cells/ml		[29-31]
Acoustic wave biosensors		10^2 to 10^5 cells/ml	<30 min	[35]

Acoustic wave sensors can act as mass-sensitive sensors, which means resonance frequency shift can be monitored via a mass load change during the reaction between

biomolecular recognition elements and the target analytes. Biomolecular recognition elements can be antibody or bacteriophage, which can capture the target analyte, such as bacteria. The parameters characterized by acoustic wave sensors are mass sensitivity or S_m, which means the immobilization of a unit mass cause a shift in resonance frequency, and quality merit factor or Q value, which means mechanical loss of sensors and reflects the sharpness of the resonance peak in the diagram about frequency shift dependence with phase. When mass sensitivity is higher, acoustic wave sensor is more sensitive. When Q quality is higher, resonance frequency shows a smaller shift.

Bibliography

[1] J. J. Gooding, Biosensor technology for detecting biological warfare agents: Recent progress and future and future trends, *Analytica Chimica Acta*, vol. 559, pp. 137-151, 2006.

[2] T. W. Alexander, T. Reuter, E. Okine, R. Sharma, and T. A. McAllister. Conventional and real-time polymerase chain reaction assessment of the fate of transgenic DNA in sheep fed roundup Ready (R) rapeseed meal, *British Journal of Nutrition*, vol. 96, pp. 997-1005, 2006.

[3] S. Horikawa. Low cost, rapid, sensitive detection of pathogenic bacteria using phage-based magnetoelastic biosensors, 2013.

[4] A. Sabelnikov, V. Zhukov, and R. Kempf. Probability of real-time detection versus probability of infection for aerosolized biowarfare agents: A model study, *Biosensors and Bioelectronics*, vol. 21, pp. 2070-2077, 2006.

[5] K. M. Hong, H. Najjar, M. Hawley, and R. D. Press. Quantitative real-time PCR with automated sample preparation for diagnosis and monitoring of cytomegalovirus infection in bone marrow transplant patients, *Clinical Chemistry*, vol. 50, pp. 846-856, 2004.

[6] K. Lind, A. Stahiberg, N. Zoric, and M. Kubista. Combining sequence-specific probes and DNA binding dyes in real-time PCR for specific nucleic acid quantification and melting curve analysis, *biotechniques*, vol. 40, pp. 315-319, 2006.

[7] B. Vogelstein, and K. W. Kinzler. Digital PCR, *Proceeding of the National Academy of Sciences of the United States of America*, vol. 96, pp. 9236-9241, 1999.

[8] J. Liu, M. Enzelberger, and S. Quake. A nanoliter rotary device for polymerase chain reaction, *Electrophoresis*, vol. 23, pp. 1531-1536, 2002.

[9] K. D. King, J. M. Vanniere, J. L. LeBlanc, K. E. Bullock, and G. P. Anderson. Automated fiber optic biosensor for multiplexed immunoassays, *Environmental Science and Technology*, vol. 34, pp. 2845-2850, 2000.

[10] F. S. Ligler, G. P. Anderson, P. T. Davidson, R. J. Foch, J. T. Ives, K. D. King, G. Page, D. A. Stenger, and J. P. Whelan. Remote Sensing using an airborne biosensor, Environmental Science & Technology, vol. 32, pp. 2461-2466, 1998.

[11] K. Tsuchiya, and C. C. Dursel. Development of a sensitive ELISA using thee monoclonal antibodies against lipopolysaccharides to detect *Xanthomonas campestris* pv. *Vesicatoria*, the causal agent of bacterial spot of tomato and pepper, *Journal of General Plant Pathology*, vol. 70, pp. 21-26, 2004.

[12] S. Horikawa. Low cost, rapid, sensitive detection of pathogenic bacteria using phage-based magnetoelastic biosensors, Dissertation in Auburn University, 2013.

[13] B. W. Blais, J. Leggate, J. Bosley, and A. Martinez-Perez. Comparison of fluorogenic and chomogenic assay systems in the detection of Escherichia coli O157 by a novel polymyxin-based ELISA, *Letters in Applied Microbiology*, vol. 39, pp. 516-522, 2004.

[14] B. Lungu, W. D. Waltman, R. D. Berghaus, and C. L. Hofacre. Comparison of a real-time RCR method with a culture method for the detection of Salmonella enterica serotype Enteritidis in naturally contaminated environmental samples from integrated poultry houses, *Journal of food protection*, vol. 75, pp. 743-747, 2012.

[15] C. Almeida, L. Cerqueira, N. Azevedo, and M. Vieira. Detection of Salmonella enterica serovar Enteritidis using real time PCR, immunocapture assay, PNA FISH and standard culture methods in differenct types of food samples, *International Journal of Food Microbiology*, vol. 161, pp. 16-22, 2013.

[16] L. P. Mansfield and S. Forsythe. The detection of Salmonella serovars from animal feed and raw chicken using a combined immunomagnetic separation and ELISA method, *Food Microbiology*, vol. 18, pp. 361-366, 2001.

[17] Z. L. Ge, M. H. Lin, P. Wang, H. Pei, J. Yan, J. Y. Shi, Q. Huang, D. N. He, C. H. Fan, and X. L. Zuo. Hybridization chain reaction amplification of MicroRNA detection with a tetrahedral DNA nanostructure-based electrochemical biosensor, Analytical Chemistry, vol. 86, pp. 2124-2130, 2014.

[18] Y. Zhang, Y. R. Yan, W.H. Chen, W. Cheng, S. Q. Li, X. J. Ding, D. D. Li, H. Wang, H. X. Ju, and S. J. Ding. A simple electrochemical biosensor for highly sensitive and specific detection of micro RNA based on mismatched catalytic hairpin assembly, *Biosensors and Bioelectronics*, vol. 68, pp. 343-349, 2015.

[19] H. L. Zou, B. L. Li, H. Q. Luo, and N. B. Li. A novel electrochemical biosensor based on hemin functionalized graphene oxide sheets for simultaneous determination of ascorbic acid, dopamine and uric acid, Sensors and Actuators B: Chemical, vol. 207, pp. 535-541, 2015.

[20] M. dos Santos, J. Agusil, B. Prieto-Simn, C. Sporer, V. Terixeira, and J. Samitier. Highly sensitive detection of pathogen *E. coli* O157:H7 by electrochemical impedance spectroscopy, *Biosensors and Bbioelectronics*, vol. 45, pp. 174-180, 2013.

[20] J. V. Rushworth, A. Ahmed, H. H. Griffiths, N. M. Pollock, N. M. Hooper, and P. A. Millner. A label-free electrical impedimetric biosensor for the specific detection of Alzheimer's amyloid-beta oligomers, *Biosensors and Bioelectronics*, vol. 56, pp. 83-90, 2014.

[21] Z. Muhammad-Tahir and E. C. Alocilja. A conductometric biosensor for biosecurity, *Biosensors and Bioelectronics*, vol. 18, pp. 813-819, 2003.

[22] G. A. Zhylyak, S. V. Dzyadevich, Y. I. Korpan, A. P. Soldatkin, and A. V. Elskaya. Application of urease conductometric biosensor for heavy-metal ion determination, *Sensors and Actuators B: Chemical*, vol. 24, pp. 145-148, 1995.

[23] A. A. Karyakin, O. A. Bobrova, L. V. Lukachova, and E. E. Karyakina. Potentiometric biosensors based on polyaniline semiconductor films, *Sensors and Actuators B: Chemical*, vol. 33, pp. 34-38, 1996.

[24] U. B. Trivedi, D. Lakshminarayana, I. L. Kothari, N. G. Patel, H. N. Kapse, K. K. Makhija, P. B. Patel, and C. J. Panchal. Potentiometric biosensors for urea determination in milk, *Sensors and Actuators B: Chemical*, vol. 140, pp. 260-266, 2009.

[25] P. D. Hale, T. Inagaki, H. I. Karan, Y. Okamoto, and T. A. Skotheim. A new class of amperometric biosensor incorporating a polymeric electron-transfer mediator, *Journal of the American Chemical Society*, vol. 111, pp. 3482-3484, 1989.

[26] P. N. Prasad. Introduction to biophotonics, *John Wiley & Sons*, Inc., 2013.

[27] J. Ju, C. Ruan, C. W. Fuller, A. N. Glazer, and R. A. Mathies. Fluorescence energy transfer dye-labeled primers for DNA sequencing and analysis, *PNAS*, vol. 92, pp. 4347-4351, 1995.

[28] http://2010.igem.org/Team:Slovenia/PROJECT/proof/studies/spr

[29] B. K. Oh, Y. K. Kim, Y. M. Bae, W. H. Lee, J. W. Choi. Detection of *Escherichia coli* O157:H7 using immunosensor based on surface plasmon resonance, *Journal of Microbiology and Biotechnology*, vol. 12, pp. 780-786, 2002.

[30] B. K. Oh, W. Lee, W. H. Lee, J. W. Choi. Nano-scale probe fabrication using self-assembly technique and application to detection of *Escherichia coli* O157:H7, *Biotechnology and Bioprocess Engineering*, vol. 8, pp. 227-232, 2003.

[31] B. K. Oh, Y. K. Kim, K. W. Park, W. H. Lee, J. W. Choi. Surface plasmon resonance immunosensor for the detection of *Salmonella* typhimurium, *Biosensors and Bioelectronics*, vol. 19, pp. 1497-1504, 2004.

[32] S. J. Martin, H. L. Bandey, and R. W. Cernosek. Equivalent-circuit model for the thickness-shear mode resonator with a viscoelastic film near film resonance, *Analytical Chemistry*, vol. 72, pp. 141-149, 2000.

[33] T. M. A. Gronewold. Surface acoustic wave sensors in the bioanalytical field: Recent trends and challenges, *Analytica Chimica Acta*, vol. 603, pp. 119-128, 2007.

[34] F. Josse, F. Bender, and R. W. Cernosek. Guided shear horizontal surface acoustic wave sensors for chemical and biochemical detection in liquids, *Analytical Chemistry*, vol. 73, pp. 5937-5944, 2001.

Chapter 3 Enhancement in the Capture Efficiency of Magnetoelastic Biosensors for *Salmonella* Using a Dilution Method

3.1 Introduction

A free-standing, phage immobilized magnetoelastic biosensor has been suggested as an economical and effective method to reduce detection time and increase the sensitivity for *Salmonella* detection [1-2]. ME biosensors have been successfully shown to detect various pathogens, for example, *Salmonella* and *E. coli*. A phage immobilized ME biosensor embraces an ME resonator platform that is covered with filamentous phage. The phage is a biomolecular recognition element and is genetically engineered to bind with its target pathogen [3-4]. The ME biosensor platform is constructed of a magnetoelastic material, which can elongate or contract along the direction of an applied external magnetic field, due to magnetostriction. Under an applied alternating magnetic field, the ME biosensor undergoes a mechanical vibration with a characteristic resonance frequency, which is based on the dimensions and materials properties of the biosensor [3, 5-6]. The oscillation of the ME biosensor leads to a magnetic signal that can be detected using a copper solenoid coil. Addition of a small mass, which is much smaller than that of the biosensor, to the surface of the biosensor causes a change in the sensor's resonance frequency, Δf [7]. When the loaded mass is larger, the resonance frequency shift will be greater [3]. In order to keep more *Salmonella* captured on the surface of the biosensor, thee different washing methods, including pipette washing, magnetic bar washing, and dilution washing, are investigated.

3.2 Materials and Methods

Filtered deionized (DI) water (pH~7.4) was used for sample washing, which was prepared using Simpak 1 Purification Pack Kit (Millipore, Billerica, MA, USA). Tris-buffered Saline (TBS) was used to maintain the pH within a relatively narrow range, which

was purchased from Thermal Fisher Scientific (USA). A 50 ml tube was used to hold a sensor during washing after loading *Salmonella*.

3.2.1 Sensor fabrication and metal deposition

A ribbon of METGLAS Alloy 2826MB was purchased from Honeywell International Company [7]. The size of 50 mm x 12.7 mm x 30 μm were cut from the ribbon and double-side polished down to a thickness of 15 μm. After polishing, the small pieces were diced into 1 mm x 0.2 mm x 15 um strip-shaped sensor platforms using an automated dicing saw. Sensors were cleaned with acetone and ethanol in an ultrasonic bath, and then successively coated with thin layers of Cr (90 nm) and Au (150 nm) using electron-beam induced deposition. The Cr layer was used as an adhesive interlayer between the Au layer and sensor platform, and the Au layer provided corrosion resistance as well as a ready surface for the phages immobilization. Finally, the sensors were annealed at 220 ℃ for 3 hours.

3.2.2 E2 phage immobilization and *Salmonella* immobilization

Each of the annealed sensor platform was immersed in a 330 μl E2 phage suspension, which was diluted from $1x10^{12}$ vir/ml to $5x10^{11}$ vir/ml using Tris-buffered saline (TBS) buffer solution, in a polypropylene PCR tube. All tubes with sensor platforms were rotated using a Barnstead LabQuake tube rotator (Fisher Scientific, Inc.) at 8 rpm for 1 h. In this way, E2 phages were allowed to attach uniformly to the platform surfaces via physical adsorption. Then, these phage-immobilized ME biosensor platforms were immersed in a $5x10^4$ *Salmonella* solution diluted from $5x10^8$ cfu/ml to $5x10^4$ cfu/ml using DI water, and rotated at 8 rpm for 1, 3, 6, 9, 12, 15, 18, 21, 24, 27, 30, 60, and 180 min. These ME biosensors were then rinsed with DI water using a dilution method in the DI water bath with 200 ml DI water, in order to remove TBS buffer components as well as loosely attached E2 phages on the platform surfaces. Finally, these ME biosensors were dried for 30 min under airing in a hood (Fisher Scientific, inc.).

3.2.3 Washing methods: pipette washing, magnetic washing, and dilution washing

The first method was pipette washing (see Fig. 2a), where DI water is pipetted into a sensor-containing tube. The biosensor was washed by a stream of DI water from a pipette, and wobbled and moved randomly, causing captured *Salmonella* to detach to a large extent by a hydrodynamic force. The second method was magnetic washing (see Fig. 2b), which was designed to wash the biosensor more gently. One magnetic bar was placed beside the tube and kept the biosensor on the inner wall of the tube. By removing the magnetic bar, the biosensor fell along the inner wall of the tube, which removes unbound or loosely bound *Salmonella*. Although more *Salmonella* could be retained on the surface of the biosensor, some bound *Salmonella* cells are still washed away via the water flowing over the surface of the biosensor. Preventing bound *Salmonella* from washing away further, dilution washing (see Fig. 2c) was applied. With this method, the biosensor was put at the bottom of an open tube. The tube was held with tweezers, and then immersed gently into a beaker filled with DI water at 1 ml per second. The tube was kept submerged for 10 seconds and transferred into a second beaker with DI water for another washing.

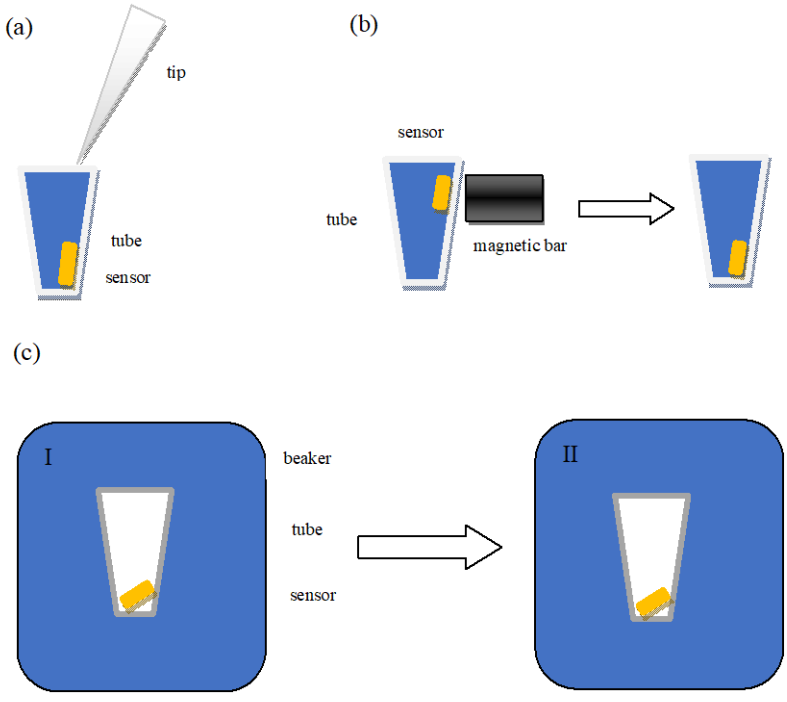

Fig. 3.1 Thee washing methods, (a) pipette washing, (b) magnetic bar washing, and (c) dilution washing.

Salmonella detection: The resonant frequency of the biosensors was measured using a measurement system consisting of a copper flat coil (from Auburn University Food Detection Center), and a network analyzer (HP/Agilent 8751A from Agilent Technologies, Inc.) operating in the S_{11} reflection mode as shown in Fig. 3.2 [8-9]. First, the biosensor was placed in the proximity of the coil in the way the longitudinal vibration of the biosensor was excited magnetically, when an incident AC signal was applied across the coil. The returned signal was compared with the incident signal over a proper range of frequencies with a span of ~100 kHz. When the largest change in normalized $|S_{11}|$ was reached due to the magneto-mechanical resonance of the biosensor, the resonant frequency of the biosensor can be determined and recorded.

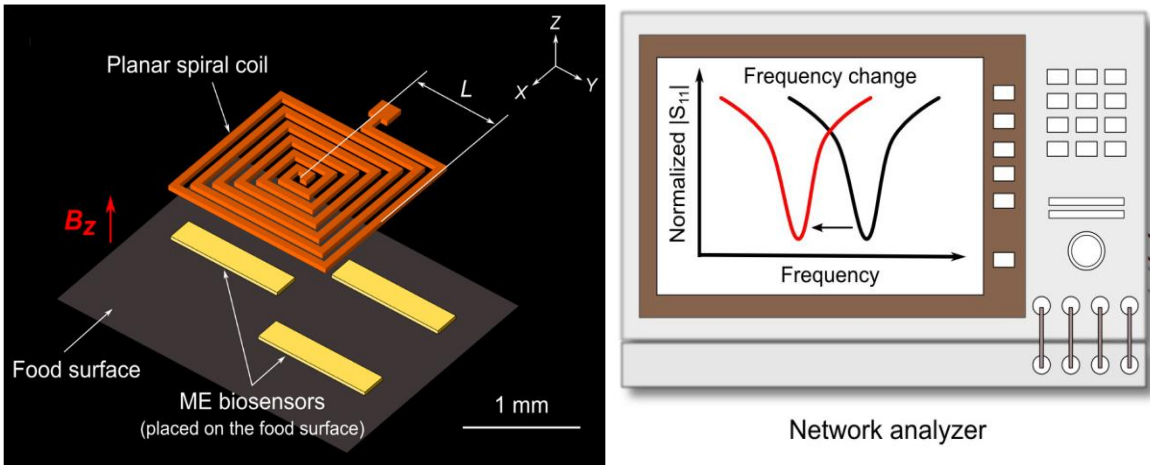

Fig. 3.2 The surface-scanning copper flat coil and network analyzer [3, 5-6]

3.3 Results and Discussions

3.3.1 Resonance frequency shift of ME biosensors after washed using pipette washing, magnetic bar washing, and dilution washing

Fig. 3.3 shows the resonant frequency shifts as a function of *Salmonella* loading time for pipette washing, magnetic bar washing, and dilution washing respectively. When mass attachment on the biosensor is uniform, the mass sensitivity of biosensor, S_m, is defined as the ratio of the resonant frequency shift, Δf, to the mass shift, Δm, which can be expressed as:

$$S_m = -\Delta f / \Delta m \qquad (1),$$

when the mass load of biosensor changed, the detected resonant frequency will be changed correspondingly. With increasing loading time, the resonant frequency shift was found to increase, and reach the plateau after 24 min, as shown in Fig. 3.3. This indicates that it took some time for the immobilized E2 phages to capture *Salmonella*, and when more and more *Salmonella* cells were captured by E2 phages, the mass shift on the biosensor increased. After 24 min, capture capacity of E2 phage has come to a maximum. In addition, the three different washing methods wash away loosely attached *Salmonella* to different extents. The dilution method kept more *Salmonella* on the biosensors compared with pipette washing and magnetic bar washing. The resonance frequency shift using dilution washing was larger than the other methods. Hence, a higher resonant frequency of the biosensor was observed with dilution washing.

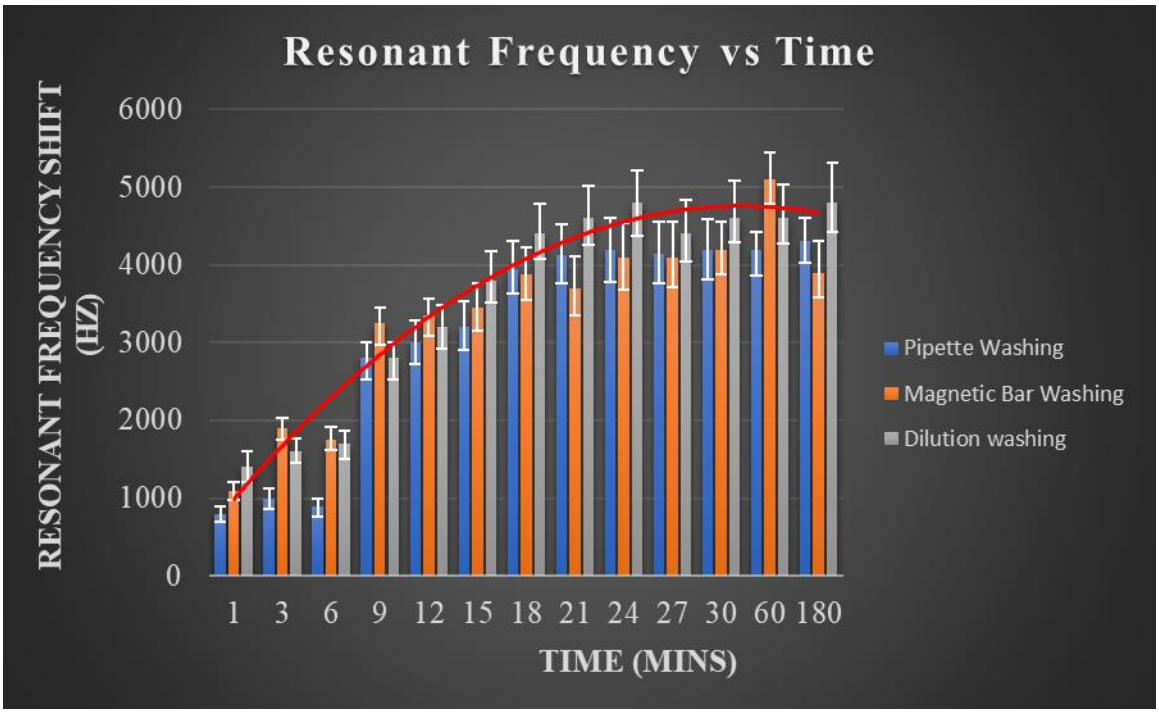

Fig. 3.3 Relationship between resonant frequency shift and loading time with *Salmonella* using pipette washing, magnetic bar washing, and dilution washing.

3.3.2 Capture efficiency of ME biosensors for *Salmonella* after washed using pipette washing, magnetic bar washing, and dilution washing

Fig. 3.4 presents the relationship between capture efficiency and loading time with *Salmonella* using pipette washing, magnetic bar washing, and dilution washing. The data is in accordance with that shown in Fig. 3.3. With binding time between *Salmonella* cells and E2 phage, thiolation E2 phage, or anti-*Salmonella* antibody increasing, more *Salmonella* were captured by E2 phages, thiolation E2 phages, or anti-*Salmonella* antibodies immobilized biosensor, which means higher capture efficiency would be obtained until the binding time between *Salmonella* cells and E2 phage, thiolation E2 phage, or anti-*Salmonella* antibodies reached 24 or 30 min. Compared with pipette washing and magnetic bar washing, dilution method washed biosensor more gently and kept more *Salmonella* cells on the biosensor.

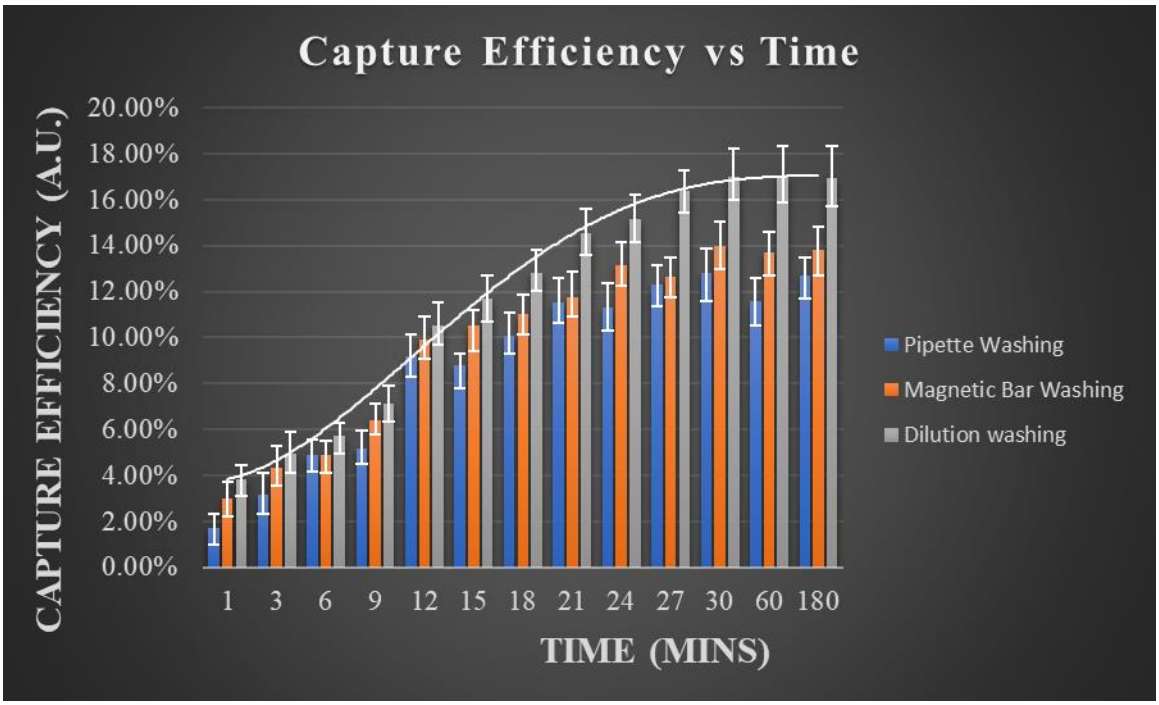

Fig. 3.4 Curve about relationship between capture efficiency and loading time with *Salmonella* using pipette washing, magnetic bar washing, and dilution washing.

3.4 Conclusions

It was found that dilution washing could protect more *Salmonella* cells from washing away due to strong oscillations caused via movement of biosensors in the DI water. Based on the variation of resonance frequency shift dependence with binding time between E2 phages and *Salmonella* cells, when binding time increased, the resonance frequency shift increased until it reached a plateau. This result indicated that it took some time to capture/bind *Salmonella* cells. Capture efficiency increased with longer binding time between E2 phage and *Salmonella* cells. After 24 min, capture capacity of E2 phages will come to a constant value, which means capture capability of E2 phages immobilized on the surface of biosensors reached saturation after 24 or 30 min. Contrasting with pipette washing and magnetic bar washing, dilution washing can increase capture efficiency of E2 phage to 17%, compared with 13% of pipette washing and 14% of magnetic bar washing.

Bibliography

[1] W. Shen, L.C. Mathison, V.A. Petrenko, B.A. Chin, "Design and characterization of a magnetoelastic sensor for the detection of biological agents," *Journal of Physics D: Applied Physics*, vol. 43, pp. 015004, 2010.

[2] Phage Ligand Sensor Devices and Uses Thereof, VA Pentrenko, VJ Vodyanoy, AM Samoylov, I Sorokulova, V. Nanduri and BA Chin, US patent 7,267, 993.

[3] Yating Chai, Shin Horikawa, Howard C. Wikle, Zhenyu Wang, and Bryan A. Chin, "Surface-scanning coil detectors for magnetoelastic biosensors: A comparison of planar-spiral and solenoid coils," Applied Physics Letters, vol.103, pp.173510, 2013.

[4] Mi-Kyung Park, Clyde H. Wikle III, Yating Chai, Shin Horikawa, Wen Shen, and Bryan A. Chin, "The effect of incubation time for Salmonella Typhimurium binding to phage-based magnetoelastic biosensors," Food Control, vol.26, pp. 539-545, 2012.

[5] Yating Chai, Shin Horikawa, Suiqiong Li, Howard C. Wikle, and Bryan A. Chin, "A surface-scanning coil detector for real-time, in-situ detection of bacteria on fresh food surfaces," Biosensors and Bioelectronics, 50, 311 (2013).

[6] Yating Chai, Howard C. Wikle, Zhenyu Wang, Shin Horikawa, Steve Best, Zhongyang Cheng, Dave F. Dyer, and Bryan A. Chin, "Design of a surface-scanning coil detector for direct bacteria detection on food surfaces using a magnetoelastic biosensor," Journal of Applied Physics, vol. 114, pp. 104504, 2013.

[7] R. Guntupalli, I. Sorokulova, E. Olsen, L. Globa, O. Pustovyy, T. Moore, B. A. Chin, J. Barbaree and V. Vodyanoy, "Detection and identification of methicillin resistant and sensitive strains of Staphylococcus aureus using tandem measurements," J. Microbiological Methods, Electronically available 6/15/2012, MIMET-03880, pgs 10, 2012 Sep;90 (3):182-91.

[8] Mi-Kyung Park, Suiqiong Li, and Bryan A. Chin, "Detection of Salmonella typhimurium grown directly on tomato surface using phage-based magnetoelastic biosensors," Food and Bioprocess Technology, vol. 6, pp. 682-689, 2013.

[9] R. Guntupalli, R. S. Lakshmanan, M. L. Johnson, J. Hu, T.-S. Huang, J. M. Barbaree, V. J. Vodyanoy, B. A. Chin. "Magnetoelastic biosensor for the detection of *Salmonella typhimurium* in food products," *Sensing and Instrumentation for Food Quality and Safety*, vol. 1, pp. 3-10, 2007.

[10] S. Huang, H. Yang, M. Johnson, J. Wan, I. Chen, V. A. Petrenko, J. M. Barbaree, and B. A. Chin, *"*Optimization of Phage-Based Magnetoelastic Biosensor Performance,*"* NSTI nanotech 2008 conference, symposium on Phage Nanobiotechnology, Boston, MA, June 1-5, 2008, Vacuum (Torr) 5 (6).

Chapter 4 Physically adsorption of E2 phage based on a magneto-elastic biosensor platform

4.1 Introduction

This chapter investigates different methods of immobilizing phage onto the ME biosensor surface and the effect of the immobilization method on the resonant frequency shift and capture efficiency. E2 phage immobilized by physical absorption and E2 phage immobilized by thiolation were investigated and compared.

Metaglas alloy magnetoelastic (ME) biosensors have been a very hot topic in sensing technologies because of their special virtues, such as wireless nature in signal transduction, high sensitivity, cost-effectiveness, and flexibility in design [1-2]. ME biosensors are based on principal called the Joule magnetostriction [3]. Under a time-varying magnetic field, the ME biosensors elastically vibrated longitudinally, which would, in turn, lead to a second magnetic field detected by a pick-up coil [4-5]. The characteristic resonance frequency of an ME biosensor is highly relative to its dimensions and the material's properties. For a strip-shaped ME biosensor with length *L*, width *W*, and thickness *T*, in which the fundamental characteristic resonant frequency of longitudinal vibration, f_0, can be expressed by Eq. (1) [4, 6]:

$$f_0 = \frac{1}{L}\sqrt{\frac{E}{p(1-v)}} \qquad (1),$$

where *E*, *p*, *v*, *L* are elastic modulus, density, Poisson's ratio of the material, and length of the biosensor, respectively. When the ME biosensor comes to contact with target pathogens, the pathogens would be captured and bound to the surface of biosensor by specific phage, which acts as the bio-molecular recognition element. A small mass change (<< the mass of biosensor) on the surface of biosensor can result in the variation of resonance frequency (Δf). The variation in resonance frequency, Δf, can be given as Eq. (2) [7]:

$$\Delta f \approx -\frac{f_0}{2}\frac{\Delta m}{M} \qquad (2),$$

where Δf, f_0, Δm, M are the change in resonance frequency, the fundamental characteristic resonance frequency of longitudinal vibration, the small mass change after contacting with target pathogens, the mass of biosensor. The variation of resonance frequency is relevant to the additional mass loaded on the surface of biosensor, which can be calculated as the number of bacterial cells bound to the surface of biosensor. The negative sign means that the resonance frequency of the ME biosensor decreases when the mass load increases. Thus, it is a very easy way to detect the resonance frequency shift, when the additional mass is loaded on the surface of biosensor.

Up to now, the current limit of detection (LOD) is 5 x 10^2 cells/ml, which is better than that in the past time. Unfortunately, there is still a risk to contaminate the foods by *Salmonella* with a lower population (<10^2 cells/ml). Therefore, it is necessary to study the physical absorption of biosensor and increase the sensitivity and specificity by enhancing bio-molecular recognition element. In this paper, the limit of detection (LOD) of 5 x 10^2 cells/ml using ME biosensors was demonstrated. In addition, morphologies of biosensors though loading E2 phage and *Salmonella* based on physical absorption was studied.

4.3 Materials and Methods

Biosensors (10 x 2 x 0.03 mm and 1 x 0.2 x 0.03 mm) were made of a ribbon of Metglas Alloy 2826MB, which were purchased from Honeywell, Morristown, USA. Filtered deionized (DI) water with PH=7.4 was used to clean the surface of biosensor and dilute the Tris-buffered Saline (TBS) solution and *Salmonella* solution, which was prepared using Simpak 1 Purification Pack Kit (Millipore, Billerica, MA, USA). Tris-buffered saline (TBS), which is purchased from Thermal Fisher Scientific in the USA, was used to maintain the PH of solution within a narrow range. Biosensors (10 x 2 x 0.03 mm) were held by sterile disposable petri dishes (35 x 10 mm), which were manufactured by VWR International, LLC, USA. Biosensors (1 x 0.2 x 0.03 mm) were loaded with E2 Phage (1x10^{12} vir/ml) and *Salmonella* (5x10^8 cfu/ml), which were provided by Dr. Tung-shi Huang's Lab, CASIC Building, Auburn University. PCR tubes with attached flat cap (0.2 ml and 1.7 ml) were purchased from Thermal Fisher Scientific, USA. TSA culture media

was made from Tryptic Soy Broth (Becton, Dickinson and Company Sparks, USA) and Agar Powder (Alfa Aesar, A Johnson Matthey Company, USA), which was used to culture *Salmonella* in the 37 ℃ incubator.

4.3.1 Sensor fabrication and metal deposition

A ribbon of Metglas 2826MB alloy, purchased from Honeywell International, was used to fabricate the Magnetoelastic (ME) biosensor platform, which will be fixed on one ultraviolet sensitive tape and diced into strips with two sizes, 10 x 2 x 0.03 mm and 1 x 0.2 x 0.03 mm, using an automatic dicing saw (DAD 3220, Disco Corporation, Japan). In order to remove tape attached with resonators, the as-diced ME resonators were exposed to Ultraviolet light with high intensity for 1 h, and then were immersed in 99.5% Acetone with ultrasonic bath to wash off the residue of tape from ME resonators. Furthermore, the residue of tape was washed off from ME resonators using 99.8% Methanol with the same procedures. Moreover, for removal of the residual stresses, which emerged during dicing process, ME resonators were annealed in vacuum (~10^{-3} Torr) at 220 ℃ for 3 hs [8]. After annealing, all ME resonators were sputter-deposited by two metal layers (Cr and Au), in which Cr layer acts as an adhesive to connect the substrate and Au layer, and Au layer serves as one corrosion resistant layer and a ready bacteria immobilization surface [9].

4.3.2 E2 phage or thiolation E2 phage immobilization and *Salmonella* immobilization

The landscape f8/8 phage library was a source for the filamentous E2 Phage or thiolation E2 phage with high specificity and selectivity towards *Salmonella* [10]. E2 phage or thiolation E2 phage for this research was prepared and provided by Dr. Tung-shi Huang's lab, Department of Biological Sciences, Auburn University. The population of as-provided E2 phage or thiolation E2 phage was 1 x 10^{12} vir/ml, and then diluted into 1 x 10^{11} vir/ml using a tris-buffered saline (TBS) solution. Every biosensor was held by one PCR tube and then immersed in the 1 x 10^{11} vir/ml E2 phage or thiolation E2 phage solution for 1 h with a rotator spinning at the rate of 8 rpm. Shin et al. found the filamentous phage can cover about 50% of the bare gold surface [11]. After immobilization, unbound E2 phage or thiolation E2 phage and salt generated from TBS solution were washed off from the surface of biosensors using DI water twice. In order to eliminate the influence of

external factors and non-specific absorption, control sensors were prepared following the above procedures, and the only difference is without E2 phage immobilization for the control ME biosensor.

4.3.3 Sample preparation for atomic force microscopy detection

For comparing the morphological difference of bare biosensor, biosensors with 10 x 2 x 0.03 mm were used, in which biosensor was divided into 3 parts: the first part was coated with nothing, the second part was loaded with 5 µl E2 phage only, and the third part was loaded with 5 µl E2 phage and 5 µl *Salmonella* successively. The first step is to wet the surface of biosensor using DI water for about 1 min and fix sensors in the mid of sterile disposable petri dishes (35 x 10 mm). And then two drips of 5 µl E2 Phage were transferred to second and third parts at the same biosensor (10 x 2 x 0.03 mm), and sensors were incubated in the rocker for 1 h at 4 rpm. After incubation, biosensors were washed using TBS solution one time and DI water twice to wash off unbound E2 phage and salt generated from TBS solution. Afterward, one drip of 5 µl *Salmonella* was transferred to the third part of the biosensor. Biosensors were incubated in the rock for 1 h at the rate of 4 rpm and then were washed using 5 µl DI water twice to remove the unbound *Salmonella*.

4.4 Results and Discussions

4.4.1 Resonance frequency shift of ME biosensors immobilized with E2 phage and thiolation E2 phage and exposed to *Salmonella*

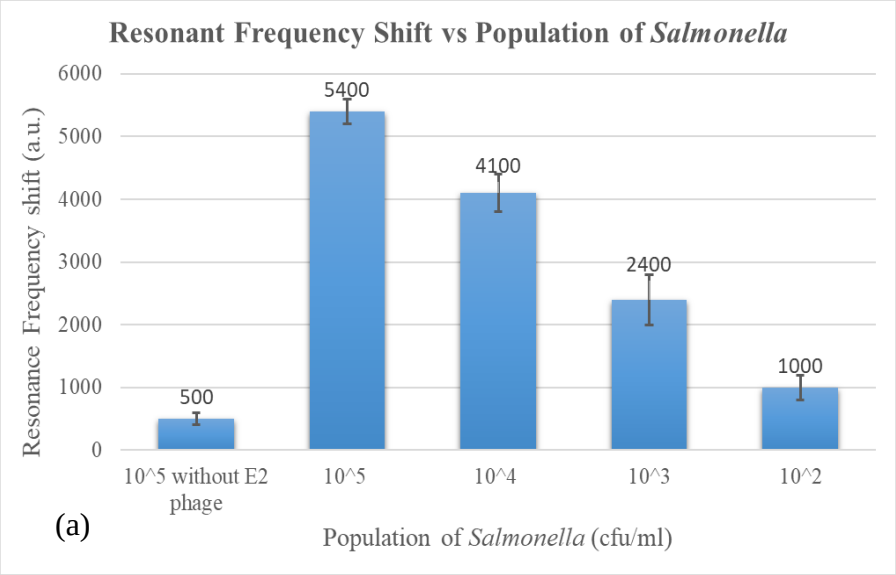

(a)

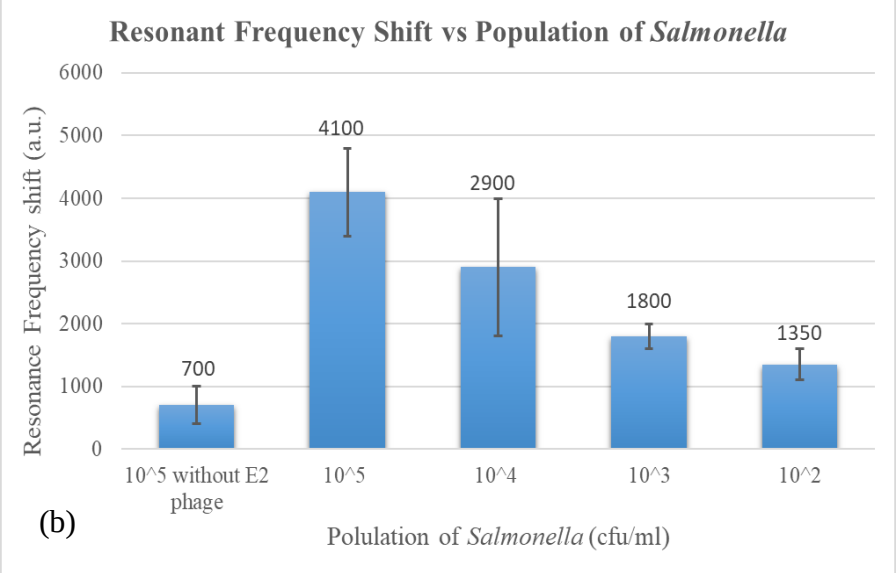

(b)

Fig. 4.1 Resonance frequency shifts of ME biosensor loading with (a) E2 phage and (b) thiolation E2 phage dependence with population of *Salmonella*. The population of both E2 phage and thiolation E2 phage was $1x10^{11}$ vir/ml, or 2.7 µg/ml which means the total molecular weight of protein within 1ml E2 phage and thiolated E2 phage, and the

population of Salmonella was from $5x10^5$ to $5x10^2$ cfu/ml. The control biosensor was one without E2 phage or thiolation E2 phage.

Fig. 4.1 shows the resonant frequency shift dependence of biosensors with a population of *Salmonella* after loading E2 Phage and thiolation E2 phage. The resonance frequency shift of ME biosensors with E2 phage and thiolation E2 phage decreased with the population of *Salmonella* ranging from 10^5 to 10^2 cfu/ml. As ME biosensor was mass sensitive, resonance frequency shift increased when mass attached to the surface of ME biosensor increased. For population of *Salmonella* from 10^5 to 10^2 cfu/ml, the amount of *Salmonella* cells captured by ME biosensors decreased, which resulted in a reduction in the resonance frequency shift. For control ME biosensor, there was a small resonance frequency shift for both E2 phage and thiolation E2 phage in Fig. 4.1 (a) and (b), which means the control biosensors had a weak capability to capture the *Salmonella* in contrast with that of biosensors with E2 phage and thiolation E2 phage. This illustrated that biosensors with E2 phage and thiolation E2 phage had a higher specificity to *Salmonella*.

4.4.2 Capture Efficiency of ME biosensors loading E2 phage and thiolation E2 phage and loading *Salmonella*

Fig. 4.2 shows the capture efficiency of biosensors loading with E2 phage and thiolation E2 phage changes with population of *Salmonella* from 10^5 to 10^2 cfu/ml. When population of *Salmonella* are 10^5 cfu/ml and 10^4 cfu/ml, the capture efficiencies are 23.87% and 20.13% for E2 Phage and 16.6% and 21.77% for thiolation E2 phage, respectively. When the population were 10^3 cfu/ml and 10^2 cfu/ml, the base value of *Salmonella* was so small that it was challenging to capture *Salmonella* cells by ME biosensors, which results in lower capture efficiencies than that for *Salmonella* of 10^5 cfu/ml and 10^4 cfu/ml. For E2 phage, the capture efficiencies were 14.27% and 12.73%, while the capture eifficiencies were 19.70% and 17.77% for thiolation E2 phage. This result was almost in agreement with that derived from the relationship between resonance frequency shift and population of *Salmonella*. When the population of E2 phage and thiolation E2 phage were very low, capture efficiencies of ME biosensors loading with E2 phage and thiolation E2 phage were

very low, which demonstrated that there was a low possibility to capture *Salmonella* cells for ME biosensors with E2 phage and thiolation E2 phage.

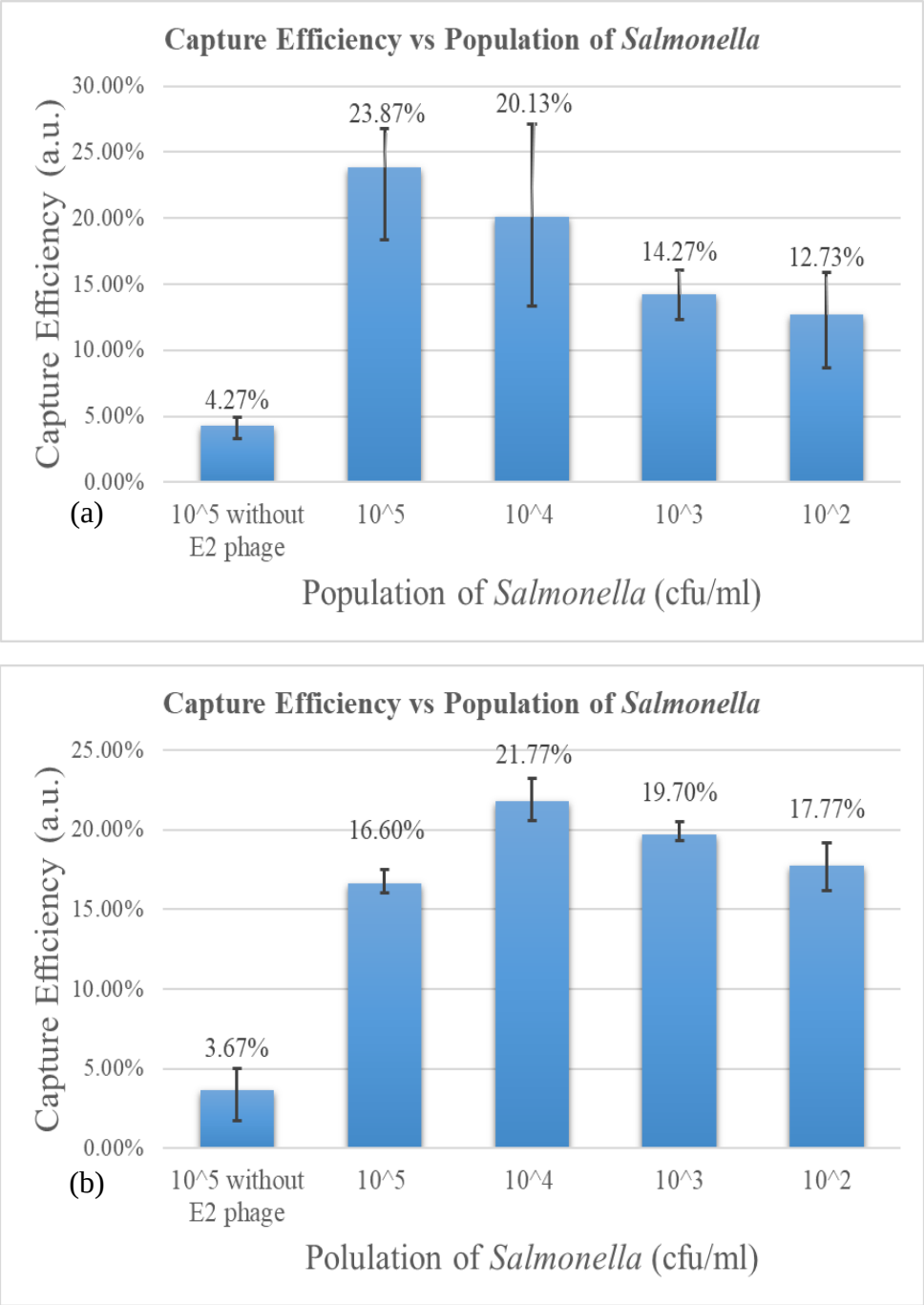

Fig. 4.2 Capture efficiencies of biosensor loading with (a) E2 phage and (b) thiolation E2 phage dependence with population of *Salmonella*, which was from $5x10^5$ to $5x10^2$ cfu/ml. The population of both E2 phage and thiolation E2 phage was $1x10^{11}$ vir/ml, or 2.7 µg/ml

which means the total molecular weight of protein within 1ml E2 phage and thiolated E2 phage, and the control biosensor was one without E2 phage or thiolation E2 phage.

4.4.3 Morphology of biosensor using a Atomic Force Microscopy

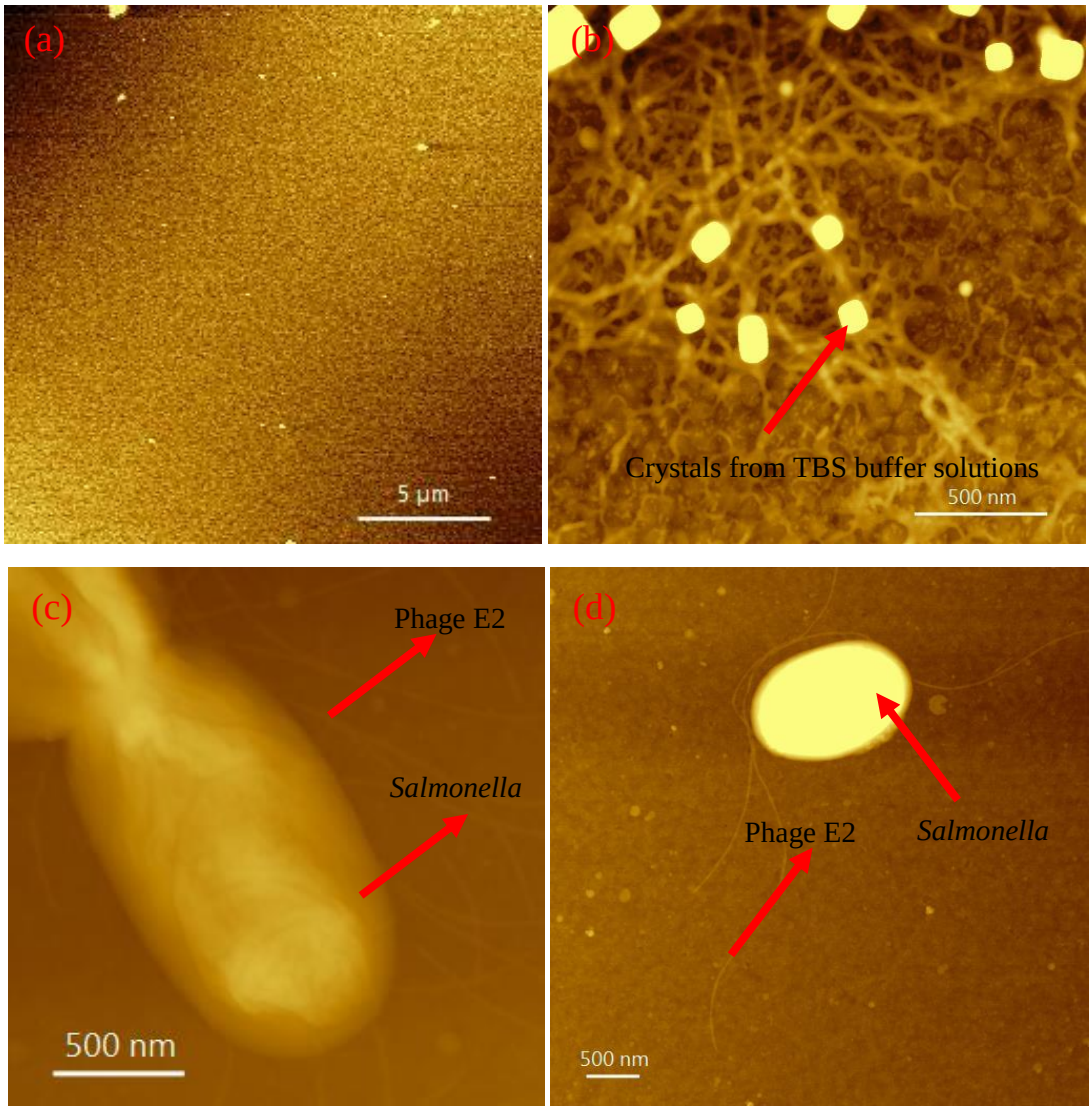

Fig. 4.3 Morphology of ME biosensors using Atomic Force Microscopy: (a) without E2 phage and *Salmonella*, (b) with E2 phage only, (c) with E2 phage and *Salmonella*, and (d) with thiolation E2 phage and *Salmonella*.

Fig. 4.3 shows morphologies of ME biosensors without E2 phage and *Salmonella*, with E2 phage only, with E2 phage and *Salmonella*, and with thiolation E2 phage and *Salmonella*. Fig. 4.3 (a) illustrates there was just one layer of uniform gold particles at the

surface of bare biosensors. When loading one layer of E2 phage only on the surface of ME biosensor, fiber-like E2 phages, shown in the Fig. 4.3 (b), crossed each other, which was in accordance with Donatan's report [12]. For cubic particles, constitution was detected by Energy Dispersive X-ray Spectroscopy (EDS), which showed these particles were NaCl crystals from TBS buffer solution in Fig. 4.4 and Table 4.1. 5 different positions were chosen to be detected for constitution, which illustrated the percent ratio of Na atoms and Cl atoms was almost 1:1 for cubic particles, while percent ratio of Na atoms and Cl atoms was 0:0 which means there were Na and Cl elements existing only in the cubic particles. Fig. 4.3 (c) and (d) shows morphology of ME biosensor with *Salmonella* cells after loading E2 phages and thiolation E2 phage. *Salmonella* cells are ellipsoidal in shape with 0.7~1.5 μm in diameter and 1~4 μm in length, while E2 phage and thiolation E2 phage were fiber-like capsid structure with length of 40 nm ~ 2 μm and diameter of about 6 nm [13].

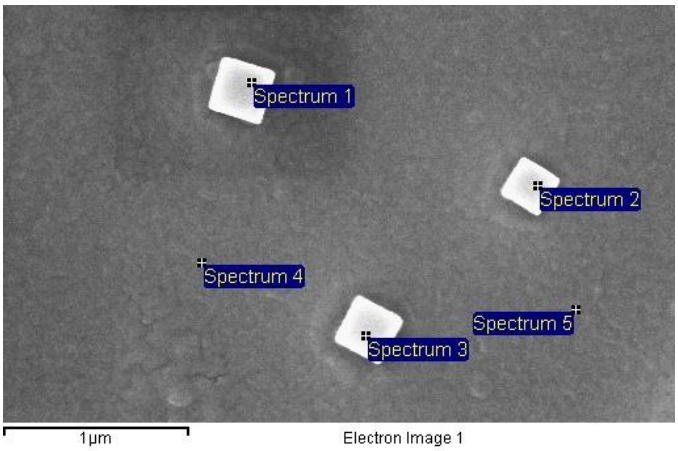

Fig. 4.4 Energy Dispersive X-ray Spectroscopy Patterns for unknown Crystals

Table 4.1 Constitution of Cubic particles (at%)

Spectrum	*Na (at%)*	*Cl (at%)*
1	55.16	44.84
2	49.65	50.35
3	48.86	51.14
4	0.00	0.00
5	0.00	0.00

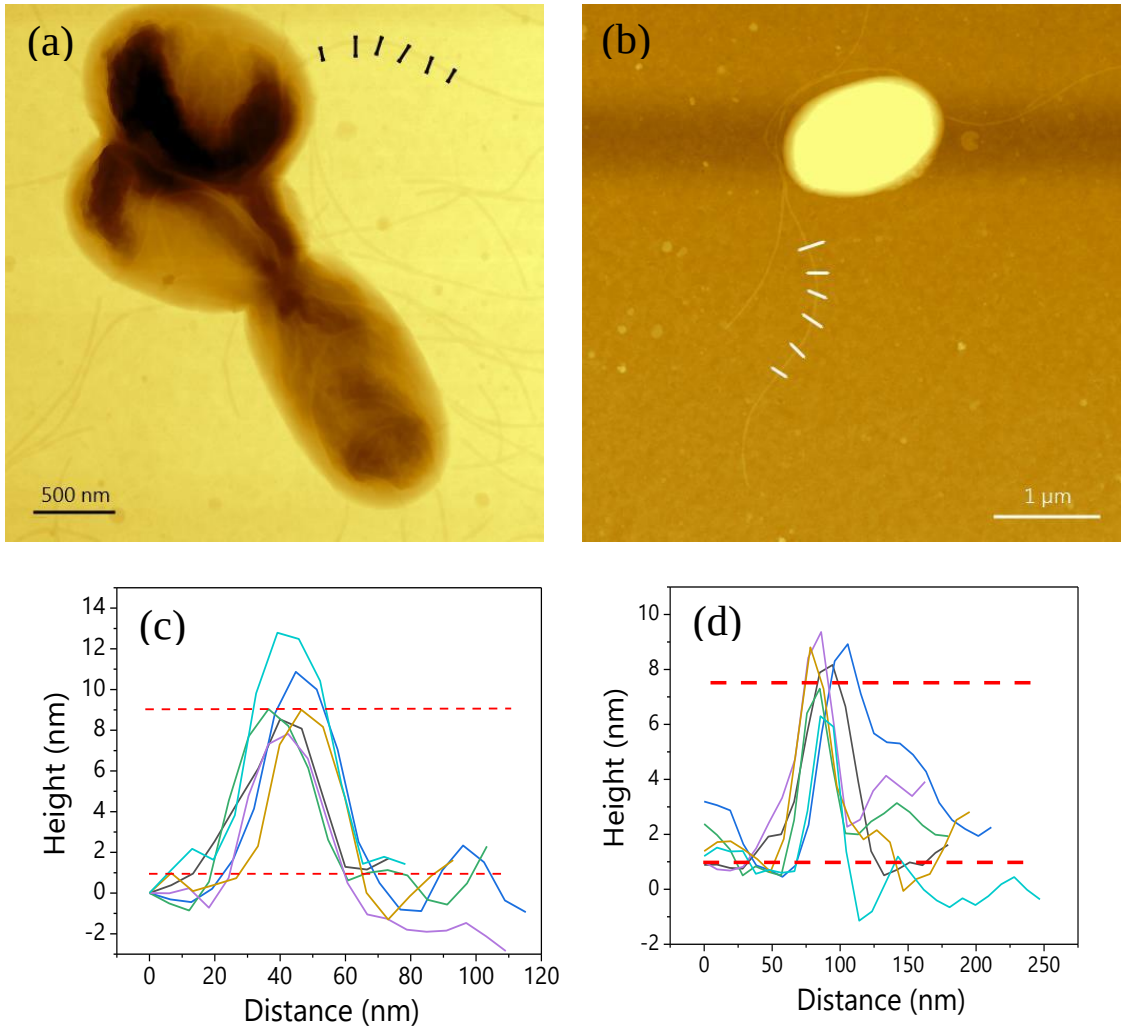

Fig. 4.5 The profile of E2 Phage on the surface of biosensor, measuring the height of one single (a) E2 phage and (b) thiolation E2 phage, and the corresponding heights of all parts of one single (c) E2 phage and (d) thiolation E2 phage.

Fig. 4.5 showed the profile of E2 phage and thiolation E2 phage on the surface of biosensor. For measuring the heights of E2 phage and thiolation E2 phage, it was necessary to choose one single E2 phage or thiolation E2 phage without crossing other phages E2 or thiolation E2 phage. Several lines were drawn on the single E2 phage or thiolation E2 phage, as shown in the Fig. 4.5 (a) and (b), to see whether the heights of all parts of E2 phage and thiolation E2 phage were equivalent, and the result illustrated the average height of one single E2 phage or thiolation E2 phage was about 7 nm, which was in agreement

with the report of Lee et al., who found the E2 phage was about 6 nm in diameter. Moreover, it could be assumed that E2 phage or thiolation E2 phage overlay on the surface of biosensor and was parallel to the biosensor surface.

4.6 Conclusions

Free-standing biosensors with E2 phage and thiolation E2 phage was prepared to study capture efficiency and resonance frequency shift using frequency analyzer and plate counting. When the population of *Salmonella* decreased from $5x10^5$ to $5\ x10^2$ cfu/ml, the resonance frequency shift decreased correspondingly, which means less *Salmonella* cells were captured when the total number of *Salmonella* reduced. In addition, capture efficiency varied from 23.87 % to 12.73 %, and from 16.60% to 17.70%, which illustrated that it was specific to *Salmonella* for E2 phage and thiolation E2 phage and it was difficult to capture *Salmonella* when ME biosensors were exposed to the low population of *Salmonella*. Though measuring the heights of E2 phage and thiolated E2 phage, it can be assumed that E2 phage or thiolated E2 phage overlay on the surface of biosensor and was parallel to the surface of biosensor.

Bibliography

[1] Y. T. Chai, S. Q. Li, S. Horikawa, M. K. Park, V. Vodyanoy, and B. A. Chin. Rapid and sensitive detection of Salmonella Typhimurium on eggshells by using wireless biosensors. *Journal of Food Protection,* 75: 631-636.

[2] S. Huang, H. Yang, R. S. Lakshmanan, M. L. Johnson, J. Wan, I. H. Chen, H. C. Wikle, V. A. Petrenko, J. M. Barbaree, and B. A. Chin. Sequential detection of Salmonella Typhimurium and Bacillus anthacis spores using magnetoelastic biosensors. *Biosensor and Bioelectronics* 24: 1730-1736, 2009.

[3] T. N. T. Dao, J. Y. Yoon, C. E. Jin, B. Koo, K. Han, Y. Shin, and T. Y. Lee. Rapid and sensitive detection of Salmonella based on microfluidic enrichment with a label-free nanobiosensing platform. *Sensors and Actuators B: Chemical* 262: 588-594, 2018.

[4] K. Zhang, L. Zhang, L. Fu, S. Li, H. Chen, Z. Y. Cheng. Magnetostrictive resonators as sensors and actuators. *Sensors and Actuators A: Physical* 200: 2-10, 2013.

[5] H. Xie, Y. T. Chai, S. Horikawa, S. Q. Li, B. A. Chin, and H. C. Wikle. A pulsed wave excitation system to characterize micron-scale magnetoelastic biosensors. *Sensors and Actuators A: Physical* 205: 143-149, 2014.

[6] C. A. Grimes, S. C. Roy, S. Rani, Q. Cai. Theory, instrumentation and applications of magnetoelastic resonance sensors: a review. *Sensors* 11: 2809-2844, 2011.

[7] P. G. Stoyanov, C. A. Grimes. A remote query magnetostrictive viscosity sensor. *Sensors and Actuators A: Physical* 80: 8-14, 2000.

[8] C. A. Grimes, K. G. Ong, K. Loiselle, P. G. Stoyanov, D. Kouzoudis, Y. Liu, C. Tong, and F. Tefiku. Magnetoelastic sensors for remote query environmental monitoring. *Smart Materials and Structures* 8: 639, 1999.

[9] S. Huang, J. Hu, J. Wan, M. Johnson, H. Shu, and B. A. Chin. The effect of annealing and gold deposition on the performance of magnetoelastic biosensors. *Materials Science and Engineering: C* 28: 380-386, 2008.

[10] M. L. Johnson, J. Wan, S. Huang, Z. Cheng, V. A. Petrnko, D. J. Kim, I. H. Chen, J. M. Barbaree, J. W. Hong, and B. A. Chin. A wireless biosensor using microfabricated phage-interfaced magnetoelastic particles. *Sensors and Actuators A: Physical* 144: 38-47, 2008.

[11] V. A. Petrenko, G. P. Smith, X. Gong, and T. Quinn. A library of organic landscapes on filamentous phage. *Protein Engneering* 9: 797-801, 1996.

[12] S. Horikawa, D. Bedi, S. Li, W. Shen, S. Huang, I. Chen, Y. Chai, M. L. Auad, M. J. Bozack, J. M. Barbaree, V. A. Petrenko, and B. A. Chin. Effects of surface functionalization on the surface coverage and the subsequent performance of phage-immobilized magnetoelastic biosensors, *Biosensors and Bioelectronics* 26: 2361-2367, 2011.

[13] S. Donatan, H. Yazici, H. Bermek, M. Sarikaya, C. Tamerler, M. Urgen. Physical elution in phage display selection of inorganic-binding peptides. *Materials Science and Engineering: C* 29: 14-19, 2009.

[14] J. W. Lee, J. W. Song, M. T. Hwang, and K. H. Lee. Nanoscale bacteriophage biosensors beyond phage display. International Journal of Nanomedicine 8: 3917-3925, 2013.

Chapter 5 Specific binding between Anti-*Salmonella* Antibody with *Salmonella*

5.1 Introduction

This chapter investigates the effects of immobilization of antibody by chemical bonding on the resonant frequency shift and capture efficiency of ME biosensors.

As one of most common foodborne pathogens, *Salmonella* is a major reason for illnesses and deaths every year, which is due to consumption of food contaminated with pathogenic bacteria [1-3]. *Salmonella* existed widespread in nature, which will result in the contamination of food during all food proceeding or at the terminal stage, such as supermarket. Generally, it will cost several days for conventional detection methods, for example, colony plate counting, which probably cause more economic losses and manpower deficiencies [4-5]. Therefore, it is critical to design a rapid, low-cost, portable method for detection of *Salmonella* contamination in food samples and environmental fields. So far, several methodologies have been used for the detection of *Salmonella*, including electrochemical detection [6], polymerase chain reaction (PCR)-based detection [7], enzyme-linked immunosorbent assay (ELISA)-based detection [8], which may also cost several hours in detection. The most challenging method is to detect exactly *Salmonella* and other pathogens real-time in the surface of sample, such as foods, feces, environmental samples, which will give inspectors a fast and specific identification for the pathogen strains in basic research and clinical diagnosis.

Polymerase chain reaction (PCR) is sensitive and rapid way to detect bacteria, but limited in reliability due to residual matrix with inhibitors, such as food components, bile salts, and urine, etc., which always influence the accuracy of detection [9-10]. The best way to improve reliability of PCR-based technique is a removal of inhibitory substances in the preparation of samples in order to detect food pathogens. By contrast, enzyme-linked immunosorbent assay (ELISA) has restrictions in the inherent instability of antibodies and high preparation cost [11-12]. Based on these defects and advantages of PCR and ELISA, it is very critical to select one specific antibody aptamer for detection of bacteria when

analyzing samples [13]. Antibodies, as one of the most common affinity-recognition elements used in biosensors, has been applied to different fields widely, including food safety, medical diagnosis, clinical analysis, and environmental monitoring [14-16]. Recently, Blackburn et al. [17] treated catalytic antibodies as an important molecular recognition element in biosensors, in which the catalytic reaction of the substrate regenerated continually the binding of sites of catalytic antibodies. Zhu et al. [18] detected α-fetoprotein using antibodies combined with nanomaterials, HP-NPs, which could have a broader detection range, while Lin et al. [19] reported immunosensor had a better limit of detection using antibody in combination with SWCNTs.

5. 1. 1 Anti-*Salmonella* Antibody

Here, antibody aptamer is a "Y" shaped molecule, including four polypeptide-two heavy chains and two light chains, as shown in Fig. 5-1 [20]. "Y" shaped antibody aptamer has different amino acid sequences at the tip for different antibodies, and these different amino acid sequences are called antigen binding sites, which consist of 110~130 amino acids and have specificity for binding antigen [21]. Fig. 6-1 shows the top part is fragment antigen binding region (FAB), which contains heavy chains, light chains, and a series of disulfide bonds, and the bottom part is fragment crystallization region (FC) [22]. Generally, FABs can respond to different antigens due to diverse regions of antibodies, while FCs just can respond some fixed antigens due to constant regions of antibodies. FABs can be used to capture diverse antigens, which range from large proteins to small molecules in size, using specific regions of antibodies [23], while the constant FC region determined the destruction mechanism of antigen. The antibodies mainly fall into five types: IgM, IgG, IgA, IgD, and IgE, according to the structure and immune function of the constant FC region.

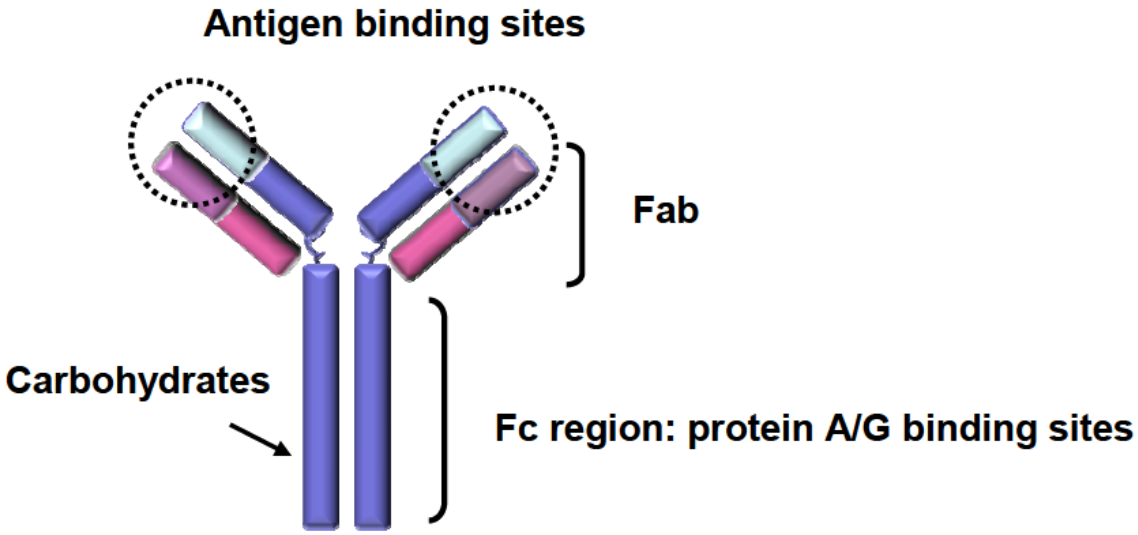

Fig. 5.1 The structural schematic diagram of antibody crystal: antigen binding sites, fragment antigen binding region, fragment crystallization region, and carbohydrates.

5.1.2 Polyclonal Antibody and Monoclonal Antibody

Based on the origins of antibody, antibody can be divided into polyclonal antibody and monoclonal antibody. Polyclonal antibodies (PAbs) are a collection of immunoglobulin molecules, originated from different B cell lineages within the body, which can react against different antigen by identifying different epitopes. The general procedure to produce polyclonal antibodies is as follow: An antigen conjugate is injected into an animal, an amplified immune response was initiated, antibodies have been created against the antigen within the body of the animal over a specific period, and blood is extracted from the animal and then purified to obtain the target antibodies. Monoclonal antibodies (MAbs) are produced from identical immune cells of one unique parent cell. In contrast with PAbs, the procedure to produce monoclonal antibodies is this: An antigen is injected into an animal to initial an immune response, B cells producing antibodies that bind to antigen are secreted from the animal, B cells are in turn fused with immortal myeloma cells, the fused B cells and myeloma cells, or hybridomas, can be screened via ELISA, the hybridomas can be cultured in a hypoxanthine-aminopterin-thymidine (HAT) medium and selected to produce one antibody per culture. Finally, the myeloma cells will initiate the localized tumor growth within the body of animal, and then the ascites with rich antibodies will be

extracted from the tumor and isolated via column chomatography [23]. Generally, it is possible to get the precise affinity for monoclonal antibodies (MAbs) due to its homogeneous nature. However, it is difficult for MAbs to estimate the affinity between antibody and antigen, because the number of antibody-antigen couples is rare. While the higher chance for polyclonal antibodies (PAbs) is to estimate the affinity of antibody and antigen, because there are more antibodies to form the antibody-antigen couple.

5.1.3 Binding between Antibody and Solid Materials

Recently, novel nanomaterials with unique physical properties, such as optical, magnetic, and mechanical properties, and chemical properties have been designed and synthesized to immobilize the biomolecules onto the solid surface. The characteristics of nanomaterials that can be used in biology and biomedicine are toxic-free, chemically and biologically stable, which may better keep biomolecules bio-active when immobilizing biomolecules onto surfaces of the nanomaterials. So far, the interaction between biomolecules and nanomaterial layers fall into 3 parts: physical binding, direct coupling reactions, and coupling reactions, as shown in Table 5. 1. These biomolecules can functionalize surfaces of metal or oxide using the methods shown in Table 5.1, and then attach to surfaces with specific conformations and in random orientations, which can cause a reduction or loss of biological activity.

Table 5.1 The types of interaction between biomolecule and nanomaterial

type	*examples*	*Reference*
Weak interaction	Hydrophobic, electrostatic, hydrogen bonding	[25]
Direct coupling reaction	EDC, sulfo-NHS, glutaraldehyde	[26]
Coupling reaction	Thiol- or silane-based SAMs	[27]

5.2 Materials and Methods

5.2.1 Preparations of some solutions

(1) Traut’s reagent

48.2 mg Traut's reagent (137.63 g/mol, 2-Iminothiolane•HCl, Pierce, 26101) powder was measured using Fisher Scientific scale with the weighing limit of 0.1 mg, and then dissolved into 15 ml filtered deionized water (DI water) from Simpak 1 Purification Pack Kit (Millipore, Billerica, MA, USA). Plate holding Traut's reagent powder must be washed 2 or 3 times, and then water was poured into 15 ml Traut's reagent solution. At last, deionized water was added into 15 ml Traut's reagent solution until the volume of solution reached 25 ml. 25 ml of 14 mM stock solution Traut's reagent was achieved and was stored at 4 ℃ freezer. The function of Traut's reagent was to thiolated the antibody.

(2) Ellman Reagent

40 mg Ellman's reagent powder, 5,5'-dithio-*bis*-(2-nitrobenzoic acid), was measured using Fisher Scientific accuSeries scale, and added into 15 ml tube. 10 ml of reaction buffer was transferred into 15 ml tube using 1000 µl pipette. The solution was vortex for 10 sec. Ellman's reagent is sensitive to -SH groups. When Ellman's reagent reacts with sulfhydryls at pH of ~7.0, high molar extinction coefficient, the solution will produce a measurable product with yellow color.

(3) Ultrapure Water

50 mg sodium azide (Fisher Chemical, USA) was measured using Fisher Scientific scale with the detection limit of 0.1 mg, and then added into an as-autoclave 500 ml bottle. Plate holding sodium azide was washed using ultrapure water, and then ultrapure water was poured into as-autoclave 500 ml bottle in the hood. 250 ml of 1 g/ml ultrapure water with 0.02% sodium azide was obtained, which was used to avoid influence of organic particles and dissolved gases, and then stored at 4 ℃ freezer.

(4) PBS buffer

1 packet of phosphate buffered saline (PBS) powder (pH=7.4, Sigma-Aldrich, USA) was poured into 1 L bottle. PBS powder in the packet was dissolved using deionized water obtained from Simpak 1 Purification Pack Kit (Millipore, Billerica, MA, USA), and then poured into 1 L bottle. Deionized water (DI water) was added into 1 L bottle until the volume of DI water reached 1 L. 1 L PBS solution with pH=7.4 was obtained, and then 1 mol/L sodium hydroxide (NaOH) was used to adjust pH value of PBS solution to 8.0 from

7.4. As-obtained PBS solution was mixed by rotator, which was used to thiolated antibody using Traut's Reagent and stored at 4 ℃ freezer.

(5) PBS buffer with 2 mM EDTA

293 mg EDTA powder (Ethylenediaminetetraacetic acid, 292.25 g/mol, VWR Chemicals, USA) was added into 500 ml bottle, and then dissolved using 500 ml PBS buffer solution. pH value of PBS buffer with 2 mM EDTA was adjusted by 1 mol/L sodium hydroxide to 8.0. Generally, EDTA could reduce the pH value of PBS buffer solution, which was used to scavenge metal ions, and was dissolved well using solution with pH=8.0. As-prepared PBS buffer solution with 2 mM EDTA need to be filtered into sterile bottle with vacuum on, and then stored at 4 ℃ freezer.

(6) Reaction Buffer Solution

6.7 g sodium phosphate (Na_3PO_4, 268.07 g/ml, Fisher Scientific, India) was dissolved into 250 ml DI water, which was 0.1 mol/L. 73.1 mg EDTA powder was dissolved into solution, and then 1 mM reaction buffer was obtained. pH value of reaction buffer solution should be adjusted into 8.0.

5.2.2 Antibody thiolation and separation

A D-Salt™ Dextran Desalting column (Pierce, Thermo Scientific, Sweden and USA) was used to separate molecules greater than 5,000 molecular weight (MW) from molecules with smaller molecular weight. One 50 ml waste tube was placed under the desalting column to hold 50 ml PBS solution (pH=8.0) with 2 mM EDTA, in which the injection volume should be the same as that volume flowing into waste tube, or 50 ml liquid waste. When the volume of PBS solution (pH=8.0) with 2 mM EDTA in the 50 ml tube remains 10 ml, anti-*Salmonella* antibody with the isotype of IgG (Abcam, ab35156, USA) was prepared. Generally, antibody was stored in -80 ℃ freezer, and brought to room temperature for use. 0.25 ml antibody and 10-fold, 20-fold, or 40-fold molar excess of 14 mM stock Traut's Reagent solution were added into 0.25 ml of PBS buffer (pH=8.0) using a 1000 µl and 20 µl pipette. The injection volumes of the stock solution are shown in Table 5-2 [28]. The as-prepared solution, including antibody, Traut's Reagent, and PBS buffer,

was mixed and the mixed solution was incubated in a rocker at the rate of 4 rpm for 1 h at room temperature.

Table 5.2 Traut's Reagent

TRAUT'S REAGENT	10-FOLD	20-FOLD	40-FOLD
VOLUME	5.35 µl	10.7 µl	21.4 µl

After about 50 minutes of incubation, PBS (pH=8.0) with 2 mM EDTA started to be added into desalting column. And then 0.5 ml fresh antibody with 14 mM Traut's Reagent solution was added below the solution level of PBS (pH=8.0) with 2 mM EDTA to prevent contamination of fresh antibody. Before separating the antibody, the bottom cap was covered so as to avoid flowing of antibody solution or waste into waste tube. 20 tubes, in which the volume is 1.7 ml, were placed under the desalting column, and were labeled from 1 to 20. After opening the bottom cap, 0.5 ml solution was held from desalting column using 1.7 ml tube. PBS (pH=8.0) solution should be added continuously from the top to avoid exposure of beads to the ambient. After obtaining 20 tubes with potential antibody solution, these 20 tubes were stored at 0 ℃ freezer. When procedures mentioned above were completed, the desalting column was washed using PBS (pH=8.0) and ultrapure water with 0.02% sodium azide.

In order to identify which of the tubes contain antibody, absorbance of each sample was measured at 280 nm using nanodrop 2000c spectrophotometer (Fisher Scientific, USA), which can be shown in Fig. 5-2. The antibodies were mainly held in the 1.7 ml tubes of 8~12. The antibodies in the 1.7 ml tubes of 8~12 were collected into one tube, and then diluted into 50 µg/ml, and fallen into different tubes, which contain 1 ml antibody solution in each tube.

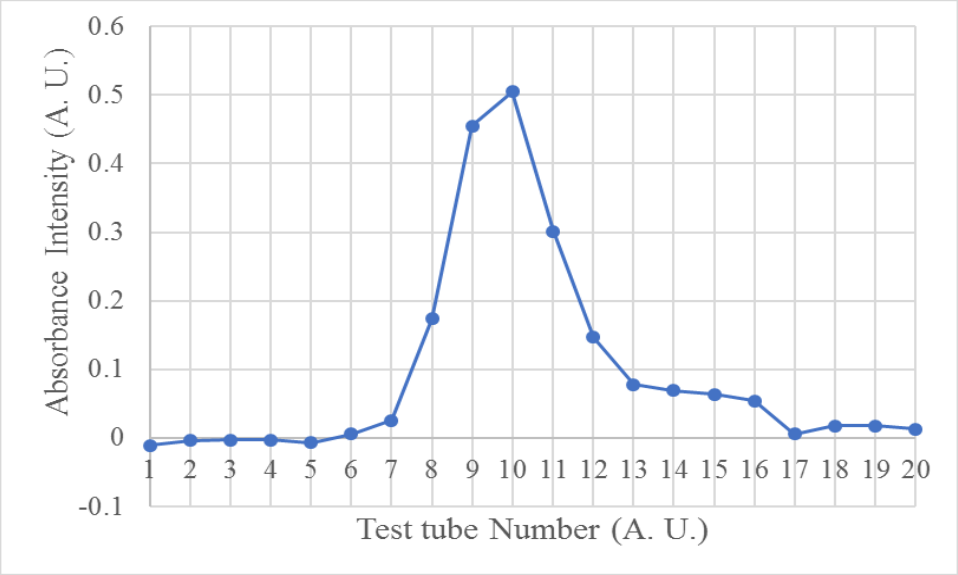

Fig. 5.2 The UV absorbance of antibody at 280 nm, which were continuous thiolated antibody samples after separation. The test number represented the number of tubes with 0.5 ml separated antibody solution.

5.2.3 Standard protein population curve

Table 5.3 Preparation of Diluted Albumin (BSA) Standards

Vial	Volume of Diluent	Volume and source of BSA	Final BSA Population
A	0	300 µl of Stock	2000 µg/ml
B	125 µl	375 µl of Stock	1500 µg/ml
C	325 µl	325 µl of Stock	1000 µg/ml
D	175 µl	175 µl of vial B dilution	750 µg/ml
E	325 µl	325 µl of vial C dilution	500 µg/ml
F	325 µl	325 µl of vial E dilution	250 µg/ml
G	325 µl	325 µl of vial F dilution	125 µg/ml
H	400 µl	100 µl of vial G dilution	25 µg/ml
I	400 µl	0	0 µg/ml=Blank

The content of Albumin (BSA) Standard (bovine serum albumin, Thermo Scientific, USA) ampule was diluted into several vials, preferably in the same diluent as the sample, according to Table 5-3 [29]. Each 1 ml ampule of Albumin Standard is sufficient to prepare a set of diluted standards for either working range suggested in Table 5-3. There will be sufficient volume for thee replications of each diluted standard solution.

25 µl of standard solution and unknown sample was added into corresponding 1.7 ml test tubes. And then 1.5 ml of the Pierce Coomassie-Dye Reagent (Thermo Scientific, USA) was added into each tube and mixed for 5 sec. Coomassie-Dye Reagent is a ready-to-use reagent, which will perform color change from brown to blue based on the amount of protein contained in the sample. With the spectrophotometer set to 595 nm, zero the instrument on a cuvette filled only with DI water. Subsequently, the absorbance of all the samples was measured. Standard curve was plotted for absorbance of Bovine Serum Albumin (Thermo Scientific, 23209. USA), which can be seen in Table 5-4, dependent with the corresponding sample, as shown in Fig. 5.3. Based on the positions of the absorbance point, the BSA standard population curve versus absorbance was obtained as shown in Fig. 5.3. X represents the absorbance values of standard samples and y represents the BSA standard population in correspondence with the absorbance value of standard sample.

Table 5.4 the absorbance of standard Bovine Serum Albumin

	Absorbance (A)
A	1.669
B	1.553
C	1.422
D	1.302
E	1.069
F	0.756
G	0.558
H	0.379
I	0.337

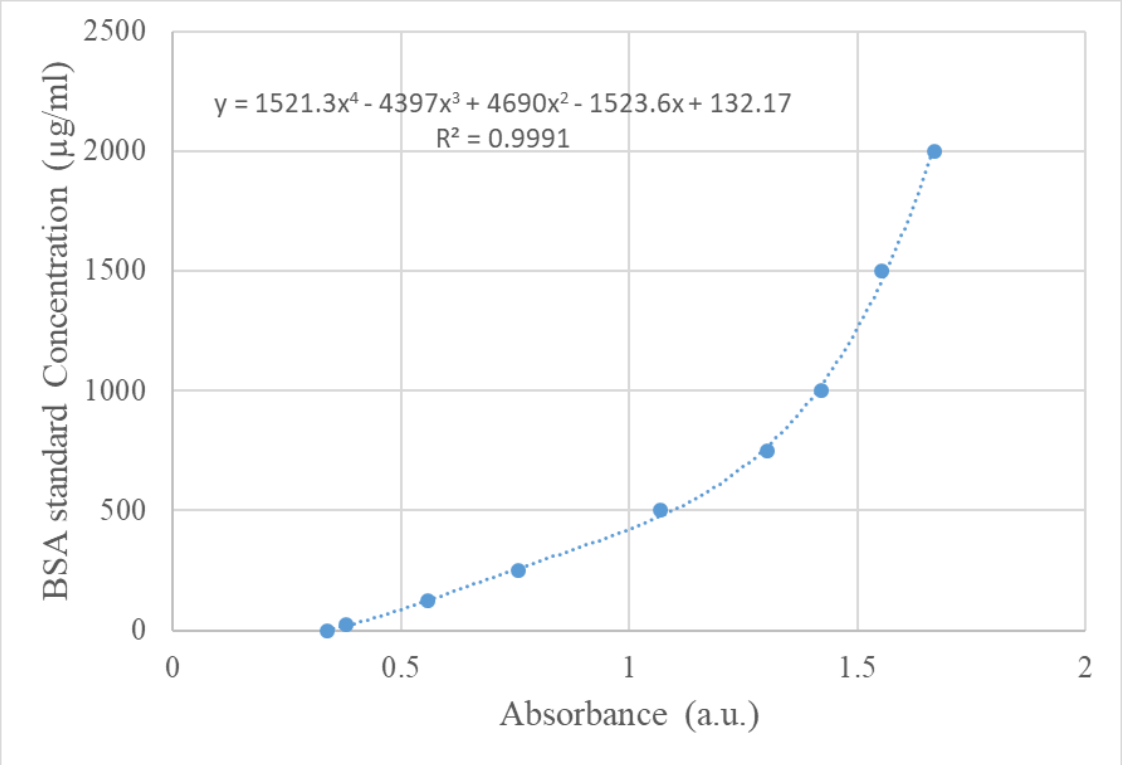

Fig. 5.3 Plot of standard BSA absorbance dependent with standard BSA population at 595 nm. The absorbance is corrected by subtracting the average blank value using DI water.

5.2.4 -SH group measured at 412 nm

50 µl Ellman's reagent buffer solution, which was prepared by mixing 4 mg Ellman's reagent (Thermo Scientific, 22582, USA) and 1 ml reaction buffer, was added into every tube of 20 tubes with 0.5 ml reaction buffer. 25 µl antibody was diluted by 10 times using DI water to form 250 µl unknown samples. Then, 250 µl unknown samples were added into corresponding tubes. Samples were mixed well and incubated at room temperature for 15 min. The absorbance of unknown samples was measured at 412 nm. The population (C) of -SH group within the samples were calculated using Beer's law:

$$C = \frac{A}{\varepsilon b} \quad (1),$$

in which C is population of -SH group, A is the absorbance of unknown sample, ε is the molar extinction coefficient, ~14,150 $M^{-1}cm^{-1}$, and b is the thickness of the cuvette (1 cm). Generally, the absorbance is proportional to the population, or when absorbance is larger,

the population of -SH group is higher. The population of antibodies and -SH groups can be shown in Table 5-5. Based on the population of antibodies and -SH groups, 20-fold anti-*Salmonella* antibodies was chosen to follow the experiments about antibodies due to higher population of antibodies and -SH groups.

Table 5.5 The population of antibodies and -SH groups within antibodies per tube which was thiolated by Traut's reagent with the 10-fold, 20-fold, and 40-fold molar excess.

	The population of antibodies	*The population of -SH groups*
10-fold	0.133 mg/ml	2.97E-06 M
20-fold	0.309 μg/ml	3.46E-06 M
40-fold	0.047 mg/ml	8.48E-07 M

5.2.5 The relationship between E2 phage and antibody

In order to confirm the population of anti-*Salmonella* antibodies, it is crucial to calculate the weight of proteins within the E2 phage, and then build the balance between weight of proteins and anti-*Salmonella* antibodies. The proteins within E2 phage contained polypeptides from gene 2, 3, 5, and 8, and so on, as shown in Table 6-6. The corresponding molecular weights of protein were found in Table 5-6. Here, the total weights of proteins are not the weight of all proteins, and the total weight of M13 bacteriophage can be treated as the total weight of all proteins within the M13 bacteriophage, which is 16.4×10^{6} Daltons in total [32]. The population of M13 bacteriophage used in previous experiment is 1×10^{11} vir/ml. The total weight of M13 bacteriophage is 2.7 μg/ml, so the population of anti-*Salmonella* antibodies used in the following experiment is 2.7 μg/ml.

Table 5.6 The molecular weight of proteins originated from different genes for one single E2 phage, in which 1 Dalton is 1.66×10^{-18} μg.

Types	*Origin*	*Molecular Weight of Protein*	*Reference*
Polypeptide	Gene 2	40,000 Daltons	[30]
A Protein	Gene 3	70,000 Daltons	[30]
The principal phage protein	Gene 5	8,000 Daltons	[30]
Major coat protein	Gene 8	1,770,000 Daltons	[31]

5.2.6 Procedures to detect the resonant frequency and capture efficiency

5.2.6.1 Resonant frequency

15 biosensors with clean surface were selected, in which C1-3 were control biosensors and M1-12 were measurement biosensors, were added into 330 µl test tubes. C1-3 were loaded with PBS (pH=8.0), and M1-12 were loaded with anti-*Salmonella* antibody of 2.7 µg/ml. All 330 µl test tubes were rotated for 1 h to load PBS (pH=8.0) onto the surface of biosensors and load anti-*Salmonella* antibody with the population of 2.7 µg/ml onto the surface of biosensors. After rotating, the biosensors were washed in the DI water and using a magnetic tweezer transferred into new, dry 330 µl test tubes. A purified Class II Biosafety Cabinet (LABCONCO, USA) was used to dry the biosensors for 30 minutes. Before using the Purified Class II Biosafety Cabinet, 75% ethyl alcohol was used to sterilize the cabinet. The resonant frequency of each biosensor was measured using the testing system and recorded at the max peak to peak value.

Salmonella with the population of $5x10^8$ cfu/ml was diluted to $5x10^5$, $5x10^4$, $5x10^3$, $5x10^2$ cfu/ml using DI water. 330 µl *Salmonella* solution with different population was loaded into corresponding tubes, as shown in Table 5-7. All tubes were rotated for 1 h, and one magnetic bar was placed in front of rotator to move biosensor up and down during rotating. The biosensors were washed using DI water and transferred into new and dry 330 µl test tubes, which were placed in the Purified Class II Biosafety Cabinet (LABCONCO,

Table 5.7 The population of *Salmonella* and anti-*Salmonella* antibody loaded into corresponding 330 µl test tubes. M means measurement biosensors and C means control biosensors.

No.	M1-3	M4-6	M7-9	M10-12	C1-3
Population of *Salmonella* (cfu/ml)	10^5	10^4	10^3	10^2	10^5
Antibody	2.7 µg/ml Anti-*Salmonella* Antibody				PBS
Time of loading Antibody	1 h	1 h	1 h	1 h	1 h
Time of loading *Salmonella*	1 h	1 h	1 h	1 h	1 h

USA) for 30 min. The resonant frequency of each biosensor was measured using the testing system and recorded at the max peak to peak value.

5.2.6.2 Capture efficiency

15 sensors with clean surface were selected. 20-fold anti-*Salmonella* antibody was diluted to 2.7 µg/ml using PBS (pH=8.0) 1x which means PBS solution was diluted by 10 times. Before loading 20-fold anti-*Salmonella* antibody, antibody was mixed gently. 12 sensors are loaded with 330 µl 20-fold Anti-*Salmonella* Antibody of 2.7 µg/ml in the 330 µl tubes. Note: to remove bubbles in the tubes and to immerse sensors adequately in the 20-fold Anti-*Salmonella* Antibody of 2.7 µg/ml. All 330 µl test tubes were rotated at the rate of 8 rpm for 1 h, and one magnetic bar was placed in front of rotor to move sensors up and down while rotating. The 3 control sensors were loaded with 330 µl PBS (pH=8.0) solution in the 330 µl test tubes, and then the same procedures were followed with the measurement sensors. At the same time, *Salmonella* ($5x10^8$ cfu/ml) was diluted into $5x10^7$ cfu/ml, and then $5x10^6$ cfu/ml, until $5x10^2$ cfu/ml, in which there were totally 165 *Salmonella* cells in the 330 µl tubes. Note: vortex *Salmonella* in every step for 3 s, and then dilute *Salmonella* by 10 times. Plate counting was used to obtain the original value of *Salmonella* with the population of $5x10^5$ cfu/ml, $5x10^4$ cfu/ml, $5x10^3$ cfu/ml, and then $5x10^2$ cfu/ml. For 10^5 and 10^4 cfu/ml, *Salmonella* needed to be diluted to 10^3 cfu/ml, and then plate counting was did based on drop assay. Sensors M1~3 and C1~3 were loaded with *Salmonella* of $5x10^5$ cfu/ml in 330 µl tubes, M4-6 were loaded with *Salmonella* of $5x10^4$ cfu/ml, M7-9 were loaded with *Salmonella* of $5x10^3$ cfu/ml, and M10-12 were loaded with *Salmonella* of $5x10^2$ cfu/ml. All test tubes were rotated for 1 h in order to bind *Salmonella* with antibodies adequately, following the procedures in Table 5-7. After loading *Salmonella*, 100 µl *Salmonella* of 10^5 and 10^4 cfu/ml was transferred into 1.7 ml tubes with 900 µl DI water to obtain *Salmonella* of 10^4 and 10^3 cfu/ml. Tubes were vortexed for 3 s, and then 100 µl *Salmonella* of 10^4 cfu/ml was transferred into 1.7 ml tubes with 900 µl DI water to obtain *Salmonella* of 10^3 cfu/ml. For 10^3, 10^4, and 10^5 cfu/ml, plate counting was did based on drop assay. For 10^2 cfu/ml, 100 µl *Salmonella* was transferred to TSA plates, and spread uniformly. All plates were incubated overnight in the 37 ℃ incubator.

5.3 Results and Discussions

5.3.1 Resonant Frequency Shift of ME Biosensor after loading Antibody

Fig. 5.4 shows resonant freqency shift of biosensors for different population of *Salmonella*. The resonant frequency shift of biosensor decreases from 4567±500 Hz to 1267±350 Hz for *Salmonella* population from 10^5 to 10^2 cfu/ml. A small change in the resonance frequency of the control bionsensors was found and is due to nonspecific binding of *Salmonella* to the sensors. The trend in resonance frequency shift is almost in agreement with those using E2 phage and thio-E2 phage.

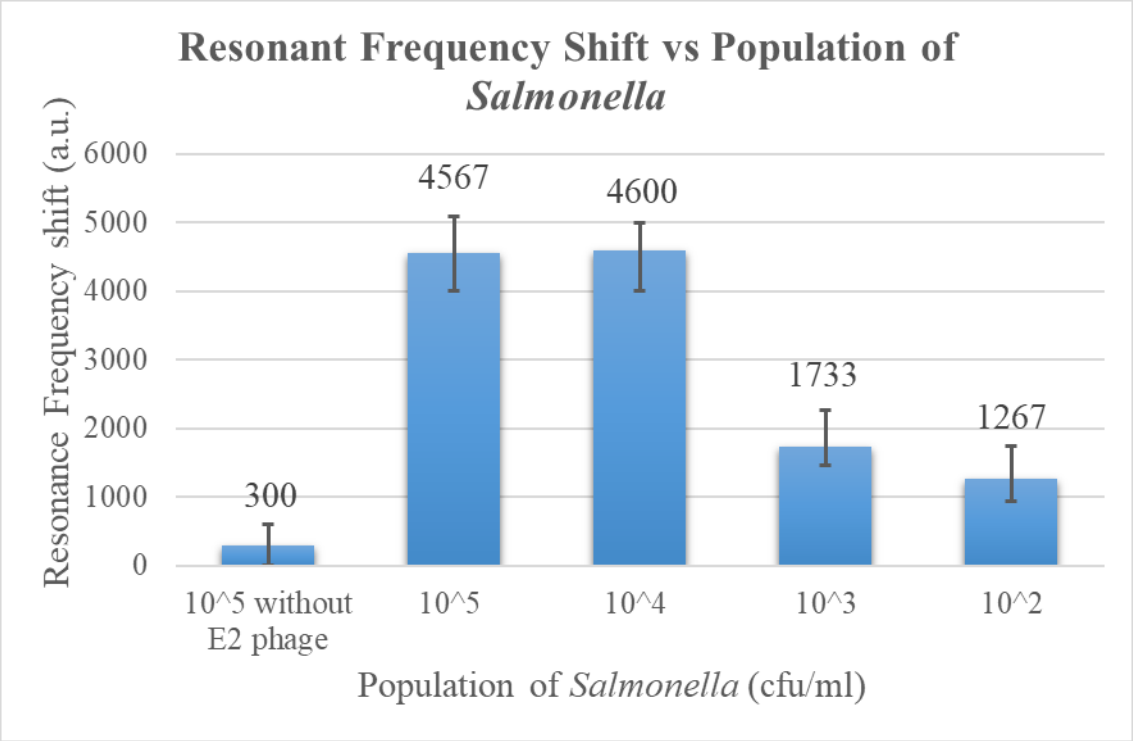

Fig. 5.4 Resonant frequency shift dependent with population of *Salmonella*, in which the population are 10^2, 10^3,10^4, 10^5 cfu/ml. The population of anti-Salmonella antibody was 2.7 µg/ml. The population of *Salmoenlla* loading on control biosensor is 10^5 cfu/ml.

5.3.2 Capture Efficiency of Biosensor with Antibody

Fig. 5.5 shows capture efficiency of biosensors loaded with anti-*Salmonella* antibody of 2.7 µg/ml and exposed to population of *Salmonella*, of 10^2, 10^3,10^4, 10^5 cfu/ml. For

population of 10^5 cfu/ml and 10^4 cfu/ml, the capture efficiencies of biosensors loaded with anti-*Salmonella* antibody were 20.73% and 12.06%, while the capture efficiencies of biosensors loaded with E2 phage and thio-E2 phage were 23.87% and 20.13%, 16.60% and 21.77%, respectively. The capture efficiency of biosensors loading with anti-*Salmonella* antibody for *Salmonella* at the low population was more than that for *Salmonella* at the high population.

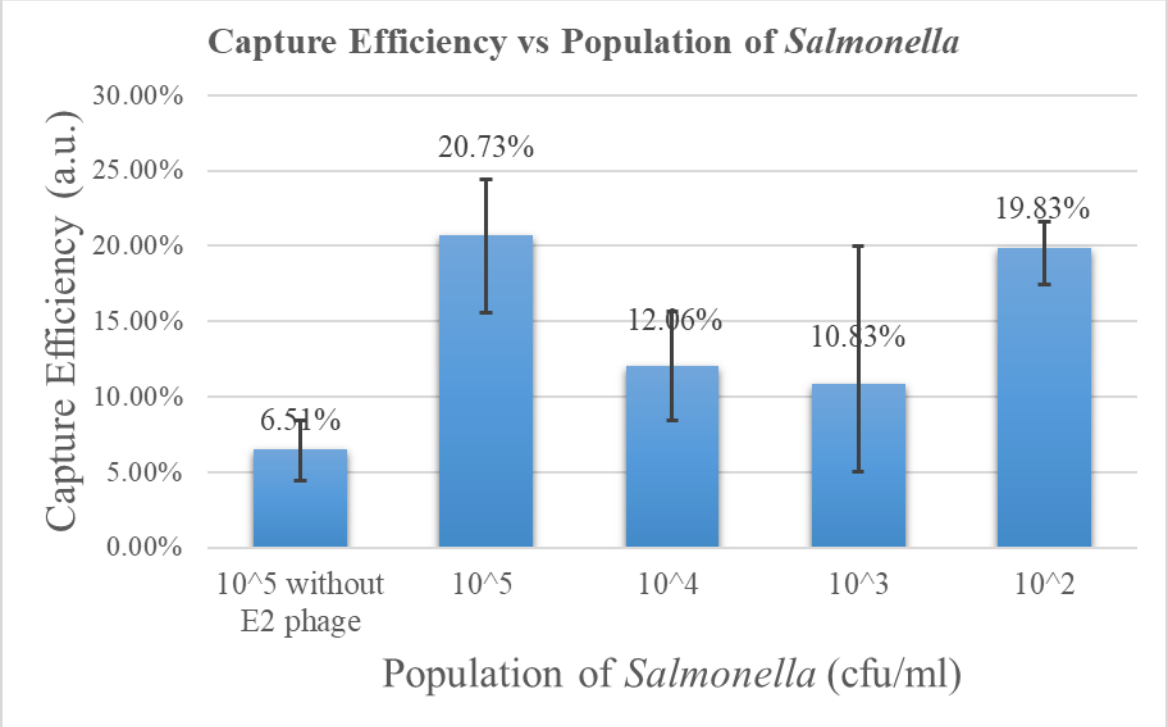

Fig. 5.5 The capture efficiency of biosensors loaded with anti-Salmonella antibody, the population of which was 2.7 µg/ml. The population of *Salmonella* were 10^2, 10^3,10^4, 10^5 cfu/ml.

5.4 Conclusions

In this chapter, sulfhydryls (-SH) were introduced into the antibody by adding Traut's Reagent. This SH linking provides a strong covalent bond between the gold and the antibody. Generally, when the amount of Traut's Reagent is larger, about 20 available primary amines may be thiolated. Additional amounts of Traut's Reagent would probably adversely the functionality of the antibody. So, it is reasonable to choose a 20-fold excess

of Traut's Reagent as the dose of thiolation for the antibody. At a population of 10^2 cfu/ml of *Salmonella*, the thiolated antibody was sensitive enough to capture *Salmonella* cells.

Bibliography

[1] D.G. Newell, M. Koopmans, L. Verhoef, E. Duizer, A. Aidara-Kane, H. Sprong, M.Opsteegh, M. Langelaar, J. Thefall, F. Scheutz, Food-borne diseases – the challenges of 20 years ago still persist while new ones continue to emerge. International Journal of Food Microbiology. vol.139 pp. S3–S15, 2010.

[2] R.L. Scharff, Economic burden from health losses due to foodborne illness in the United States, Journal of Food Protection, vol. 75, pp. 123–131, 2012.

[3] G.S. Chilcott, K.T. Hughes, Coupling of flagellar gene expression to flagellar assembly in *Salmonella* enterica serovar Typhimurium and Escherichia coli, Microbiology and Molecular Biology Reviews, vol. 64, pp. 694–708, 2000.

[4] A.S. Afonso, B. Pérez-López, R.C. Faria, L.H.C. Mattoso, M. Hernández-Herrero, A.X. Roig-Sagués, M. D. Costa, A. Merkoci, Electrochemical detection of *Salmonella* using gold nanoparticles, Biosensors and Bioelectronics, vol. 40, pp. 121–126, 2013.

[5] M. Dilmaghani, M. Ahmadi, T. Zahaeisalehi, A. Talebi, Detection of Salmonellaenterica serovar Typhimurium from avians using multiplex-PCR, Veterinary Research Forum, vol. 2, pp. 327-338, 2011.

[6] M. E. Arnold, J. J. Carriquemas, I. Mclaren, R. H. Davies, A comparison of pooled and individual bird sampling for detection of Salmonella in commercial egg laying flocks, Preventive Veterinary Medicine, vol. 99, pp. 176–184, 2011.

[7] B.W. Brooks, C.L. Lutze-Wallace, J. Devenish, M. Elmufti, T. Burke, Development of an antigen-capture monoclonal antibody-based enzyme-linked immunosorbent assay and comparison with culture for detection of Salmonella enterica serovar enteritidis in poultry hatchery environmental samples, Journal of Veterinary Diagnostic Investigation: Official Publication of the American Association of Veterinary Laboratory Diagnosticians, Inc., vol. 24, pp. 509-515, 2012.

[8] B. Kokoskova, J. D. Janse, Enzyme-linked immunosorbent assay for the detection and identification of plant pathogenic bacteria (in particular for Erwinia amylovora and

Clavibacter michiganensis subsp. sepedonicus), Methods in Molecular Biology, vol. 508, pp. 75-87, 2009.

[9] S.R. Han, S.W. Lee, In vitro selection of RNA aptamer specific to Salmonella typhimurium, Journal of Microbiology and Biotechnology, vol. 23, pp. 878–884, 2013.

[10] J. Yuan, Z. Tao, Y. Yu, X. Ma, Y. Xia, L. Wang, Z. Wang, A visual detection method for Salmonella Typhimurium based on aptamer recognition andnanogold labeling, *Food Control*, vol. 37, pp. 188-192, 2014.

[11] M. Girardot, H.Y. Li, S. Descroix, A. Varenne, Determination of binding parameters between lysozyme and its aptamer by frontal analysis continuous microchip electrophoresis (FACMCE), *Journal of Chomatography A*, vol. 1218, pp. 4052–4058, 2011.

[12] X. Lin, Q. Chen, W. Liu, L. Yi, H. Li, Z. Wang, J.M. Lin, Assay of multiplexproteins from cell metabolism based on tunable aptamer and microchipelectrophoresis, *Biosensors and Bioelectronics*, vol. 63, pp. 105–111, 2015.

[13] L. Hao, Y. Bai, H. Wang, Q. Zhao, Affinity capillary electrophoresis with laser induced fluorescence detection for thombin analysis using nuclease-resistant RNA aptamers, *Journal of Chomatography A*, vol. 1476, pp. 124-129, 2016.

[14] C. I. L. Justino, T. A. Rocha-Santos, A. C. Duarte. Review of analytical figures of merit of sensors and biosensors in clinical applications. *Trends in Analytical Chemistry*, vol. 10, pp. 1172-1183, 2010.

[15] C. I. L. Justino, A. C. Freitas, J. P. Amaral, T. A. P. Rocha-Santos, S. Cardoso, A. C. Duarte. Disposable immunosensors for C-reactive protein based on carbon nanotubes field effect transistors. Talanta, vol. 108, pp. 165-170, 2013.

[16] C. I. L. Justino, K. Duarte, S. Lucas, P. Chaves, P. Bettencourt, A. C. Freitas, et al.. Assessment of cardiovascular disease risk using immunosensors for determination of C-reactive protein levels in serum and saliva: a pilot study, Bioanalysis, vol. 6, pp. 1459-1470, 2014.

[17] G. F. Blackburn, D. B. Talley, P. M. Booth, C. N. Durfor, M. T. martin, A. D. Napper, and A. R. Rees. Potentiometric biosensor employing catalytic antibodies as the molecular recognition element. *Analytical Chemistry*, vol. 62, pp. 2211-2216, 1990.

[18] Q. Zhu, R. Yuan, Y. Chai, J. Han, Y. Li, N. Liao. A novel amperometric immunosensor constructed with gold-platinum nanoparticles and horseradish peroxidase nanoparticles as well as nickel hexacyanoferrates nanoparticles, *Analyst*, vol. 138, pp. 620-626, 2013.

[19] J. Lin, Z. Wei, H. Zhang, M. Shao. Sensitive immunosensor for the label-free determination of tumor marker based on carbon nanotubes/mesoporous silica and graphene modified electrode. *Biosensors and Bioelectronics*, vol. 41, pp. 342-347, 2013.

[20] Y. Jung, J. Y. Jeong, B. H. Chung. Recent advances in immobilization methods of antibodies on solid supports. Analyst, vol. 133, pp. 687-701, 2008.

[21] S. S. Iqbal, M. W. Mayo, J. G. Bruno, B. C. Bronk, C. A. Batt, J. P. Chambers. A review of molecular recognition technologies for detection of biological theat agents. Biosensors and Bioelectronics, vol. 15, pp. 549-578, 2000.

[22] J. S. Garvey, N. E. Cremer, D. H. Sussdorf, 1977. Methods in immunology, W. A. Benjamin, Inc., Reading, Massachusetts.

[23] G. Kohler, C. Milstein. Continuous cultures of fused cells secreting antibody of predefined specificity, Nature, vol. 256, pp. 495-497, 1975.

[24] N. S. Lipman, L. R. Jackson, L. J. Trudel, and F. W. Garcia. Monoclonal versus polyclonal antibodies: distinguish characteristics applications, and information resources. ILAR Journal, vol. 46, pp. 258-268, 2005.

[25] S. Santra, P. Zhang, K. Wang, R. Tapec, and W. H. Tan. Conjugation of biomolecules with luminophore-doped silica nanoparticles for photostable biomarkers, *Analytical Chemistry*, vol. 73, pp. 4988-4993, 2001.

[26] D. Bartczak, and A. G. Kanaras. Preparation of peptide-functionalized gold nanoparticles using one pot EDC/sulfo-NHS coupling, Langmuir, vol. 27, pp. 10119-10123, 2011.

[27] S. K. Arya, A. K. Prusty, S. P. Singh, P. R. Solanki, M. K. Pandey, M. Datta, and B. D. Malhotra. Cholesterol biosensor based on N-(2-aminoethyl)-3-aminopropyl-trimethoxysilane self-assembled monolayer, Analytical Biochemistry, vol. 363, pp. 210-218, 2007.

[28] L. L. Fu, Development of phage/antibody immobilized magnetostrictive biosensors, 2010.

[29] https://www.thermofisher.com/order/catalog/product/22582

[30] T. J. Henry, and D. Partt. The proteins of bacteriophage M13, PNAS 62, 800-807, 1969.

[31] S. A. Berkowitz, and L. A. Day. Mass, Length, Composition and structure of the filamentous bacterial virus fd. Journal of Molecular Biology, 102, 531-547, 1976.

[32] S. D. Branston. An investigation of the properties of bacteriophage M13 and the implications for its large-scale bioprocessing.

Chapter 6 Conclusions

This research employs wireless magnetoelastic biosensors to detect *Salmonella* rapidly and directly, and plate counting for quantitative detection to confirm biosensor results. Magnetoelastic biosensors were investigated using thee different biomolecular recognition element/immobilization pairs: 1) physically absorbed E2 phage, 2) SH linked E2 phage, and 3) SH linked anti-*Salmonella* antibody.

Thee different washing methods were compared to determine the effect of washing on bound cells. It was found that dilution washing retained more bound *Salmonella* cells than the other two techniques by avoiding subjecting the biosensors to strong streams of DI water and oscillations of the biosensors in the DI water. Comparing dilution washing, pipette washing, and magnetic bar washing, the techniques yielded capture efficiencies of 17%, 14% and 13% respectively.

It was found that increasing the time of exposure of the biosensors to the *Salmonella* solution, could increase both the resonant frequency shift and capture efficiency. Eventually the increase in resonant frequency shift and capture efficiency reaches a maximum indicating there is no advantage to increasing the time of exposure of the biosensors to the *Salmonella* solution. The optimum time for exposure to *Salmonella* bacteria was between 24 and 30 minutes.

For thiolation, sulphydryls (-SH) were introduced into antibody via adding Traut's Reagent, which was used to immobilize anti-*Salmonella* antibody on the magnetoelastic

sensors via covalent bonding between sulphydryls and gold. Considering the population of antibody and sulphydryls, it is reasonable to choose a 20-fold excess of Traut's Reagent as the dose of thiolation of antibody.

In order to obtain a highly efficient molecular recognition element, free-standing magnetoelastic biosensors with E2 phage, thiolated E2 phage, and anti-*Salmonella* antibody were prepared to study capture efficiency using plate counting and resonance frequency shift using network analyzer. When the population of *Salmonella* decreased from $5x10^5$ to $5 x10^2$ cfu/ml, the resonance frequency shift of E2 phage, thiolated E2 phage, and anti-*Salmonella* antibody decreased correspondingly. In addition, capture efficiency of E2 phage decreased from 23.87 % to 12.73 %, and for thiolated E2 phage, the capture efficiency was almost a constant value (~18.96 %). For anti-*Salmonella* antibody, a higher capture efficiency (~19.83 %) was measured when ME biosensors were exposed to a low population of *Salmonella*. The results of these experiments indicate that E2 phage immobilized by physical absorption, provided the best overall capture efficiency and resonant frequency changes.

AFM measurements were used to compare and contrast E2 phage immobilized onto the surface of the ME biosensors. These AFM measurements demonstrated that both the physically absorbed and thiolated E2 phage are immobilized onto the ME biosensor surface and are positioned flat (parallel) to the surface. Most *Salmonella* cells were found to be bound by several phages on the ME biosensor surface.